Molecular Polarizability as a Descriptor for Molecular Conductance

by

Reza Vatan Meidanshahi

A Thesis Presented in Partial Fulfillment
of the Requirement for the Degree
Master of Science

Approved November 2014 by the
Graduate Supervisory Committee:

Vladimiro Mujica, Chair
Andrew Chizmeshya
Ranko Richert

ARIZONA STATE UNIVERSITY

December 2014

ABSTRACT

We studied the relationship between the polarizability and the molecular conductance that arises in the response of a molecule to an external electric field. To illustrate the plausibility of the idea, we used Simmons' tunneling model, which describes image charge and dielectric effects on electron transport through a barrier. In such a model, the barrier height depends on the dielectric constant of the electrode-molecule-electrode junction, which in turn can be approximately expressed in terms of the molecular polarizability via the classical Clausius-Mossotti relation. In addition to using the tunneling model, the validity of the relationships between the molecular polarizability and the molecular conductance was tested by comparing calculated and experimentally measured conductances of different chemical structures ranging from covalent bonded to non-covalent bonded systems. We found that either using the tunneling model or the first-principle calculated quantities or experimental data, the conductance decreases as the molecular polarizability increases. In contrast to this strong correlation, our results showed that in some cases there was a weaker or none correlation between the conductance and other molecular electronic properties including HOMO-LUMO gap, chemical geometries, and interactions energies. All these results together suggest that using the molecular polarizability as a molecular descriptor for conductance can offer some advantages compared to using other molecular electronic properties and can give additional insight about the electronic transport property of a junction.

These results also show the validity of the physically intuitive picture that to a first approximation a molecule in a junction behaves as a dielectric that is polarized in the opposite sense of the applied bias, thereby creating an interfacial barrier that hampers tunneling. The use of the polarizability as a descriptor of molecular conductance offers significant conceptual and practical advantages over a picture based in molecular orbitals. Despite the simplicity of our model, it sheds light on a hitherto neglected connection between molecular polarizability and conductance and paves the way for further conceptual and theoretical developments.

The results of this work was sent to two publications. One of them was accepted in the International Journal of Nanotechnology (IJNT) and the other is still under review in the Journal of Physical Chemistry C.

To my family and friends

and to all my those teachers who gave me motivation and enthusiasm for learning.

ACKNOWLEDGEMENTS

Finishing this work would never have been possible without many people that helped me, motivated me, guided me and believed in me.

First, I would like to express my deep gratitude to my advisor, Dr. Vladimiro Mujica, for his support, guidance and help during my master degree.

I would like to express my very special thanks to Dr. Pilarisetty Tarakeshwar for all his immense support and for providing me an opportunity to learn many things and to work with different people under his supervision. Without his motivation, his help, and his kindness my research would not have been ever possible. He was a constant source of support and hope during my work.

I would like to thank Dr. Julio L. Palma for spending his valuable time to teach me some software and to discuss with me during the data analysis.

I would also like to thank my lab-mates Shobeir and Micah.

A special thanks to all my friends for their help, their encouragement, and their suggestions.

Finally, I would like to express my special gratitude to my family for their immense love, support and care. Without them, completing this or any other endeavour in my life would never have been possible.

TABLE OF CONTENTS

Page

CHAPTER Page

LIST OF TABLES

Table Page

LIST OF FIGURES

Figure Page

Figure Page

Chapter 1

INTRODUCTION

The idea of using individual molecules as active components in nano-electronic devices was first introduced by A. Aviram and M. Ratner in 1974 in theoretically explaining the I-V property of π molecular system as a potential rectifier (Aviram et al., 1974). From that time until now, there has been many studies and researches in exploring, modelling, and interpreting the electron transport properties of different single molecules (Cui et al., 2001; Smit et al., 2002; Xu, et al., 2003; Reed, et al., 1997; Porath, et al. 2000; Evers et al. 2004; Stokbro et al. 2003; Lang, 1988; Tersoff et al., 1993; Imry, 1997; Miller, 1975; Miller, 1983; Galperin et al., 2005; Mujica et al., 1996; de Andrade, 1998). One of the main focuses of these studies has been on determining and interpreting molecular conductance which can represent the most aspects of the electron transport properties of a molecule (Chen et al., 2007). Despite many difficulties in both experimental and theoretical work, researchers have recently made a remarkable advances in determining molecular conductance. In this chapter, a brief overview of these developed experimental methods and advanced theoretical frameworks in measuring and interpreting molecular conductance will be provided.

This chapter is organized as fallows: first the experimental methods for measuring the molecular conductance will be explained briefly. Second, the fundamental aspects of theoretical framework used in this study for computing conductance values and driving our model will be discussed in detail. Finally, a brief overview of the

work done on the connection between the intrinsic electronic property of a molecule and its conductance will be provided. In this section, I will also briefly discuss the possible connection between polarizability and conductance.

1.1 Experimental Methods to Measure Molecular Conductance

For measuring the conductance of a molecule, one should first fix the molecule between two electrodes as seen in Figure 1.1 (Chen et al., 2007). The measured molecular conductance with the described experimental set up is not only dependent on the molecule itself but also dependent on the electrodes, the geometry and the chemical nature of the contact, the temperature, and the environment (Kalakodimi et al., 2006; Xue et al., 2003; San-Huang et al., 2004; Mller, 2006; Beebe et al., 2002; Hu et al., 2005; Basch et al., 2005; Schmickler et al., 1992; Kuznetsov et al., 1992; Weiss et al., 2005; Nitzan, 2001; Selzer et al., 2004; Haiss et al., 2006; Di Ventra et al., 2001). Controlling all these parameters (especially the molecule-electrode contacts) in order to get reproducible conductance values have been a challenge for many years that experimentalists faced to (Cui, 2001; Magoga, 1997; Yaliraki, 1999; Moresco, 2003). Experimental techniques that have been developed over the past decades to overcome these challenges are divided into two main categories: 1) the molecular film measurement technique and 2) single-molecule measurement technique. In following sections, these two methods will be briefly explained.

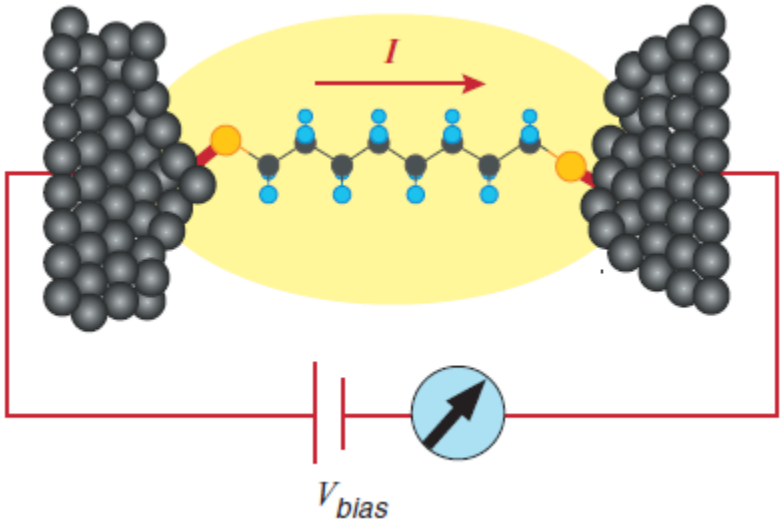

Figure 1.1: Experimental Set-up for Molecular Conductance Measurements (Chen et al., 2007).

1.1.1 Molecular Film Measurement

In molecular film measurements, first a layer or several of fairly ordered molecules is placed on the surface of one of the electrodes (Figure 1.2) via self-assembly or Langmuir-Blodgett methods (Mantooth et al., 2003; Metzger, 2003). Then the second electrode is brought to the top of the molecular film, and the electrical current in external circuit under different applied voltage is measured in order to determine the conductance of the molecular film. Using this method, the exact ordering of the molecules next to each other for making a monolayer or multi-layer molecular film is strongly desired for successful measurements and data interpretation. The most challenging part of this experiment is placing the second electrode on the top of the molecular film without having a short circuit between the top electrode and bot-

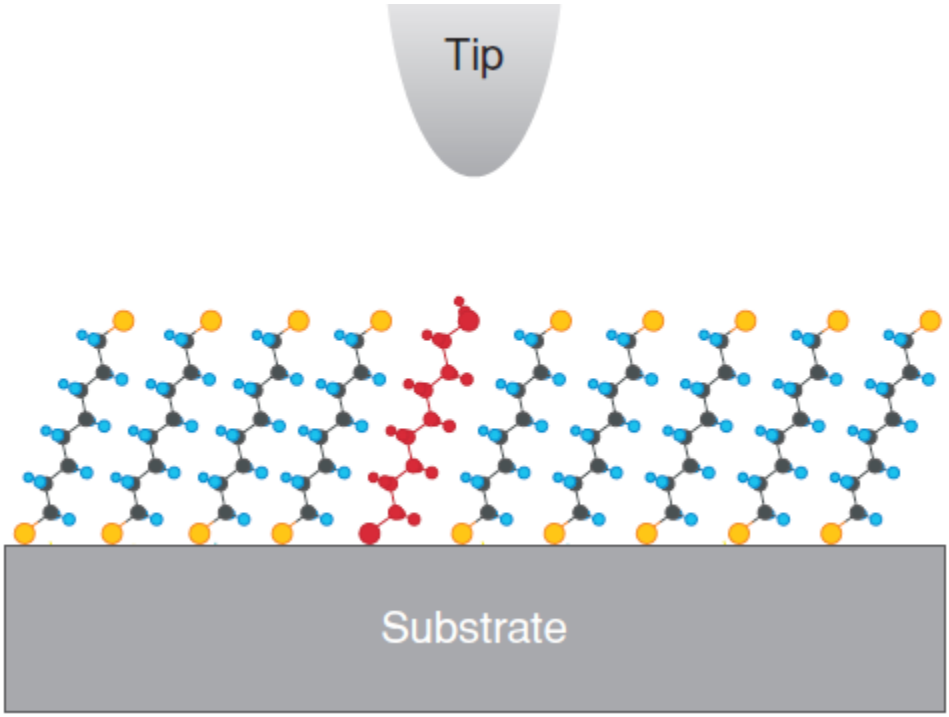

Figure 1.2: Experimental Set-up for Molecular Film Conductance Measurements (Chen et al., 2007).

tom electrode. The conductance values obtained from this experiment describe the conductance of a group of many single molecules, although one can reduce the number of involved molecules in conductance measurement by using nanoelectrodes or nanopores fabricated in bottom electrode. The molecular film conductance measurement has had a great impact on our understanding of the electron transport properties of molecules and their function in nano-electronic devices as switches, rectifiers, and resistors. There are some important criteria for this measurement that should be considered: 1) this method can be only used for molecules that are able to form a well ordered molecular film 2) inherent defects or induced defects due to fabrication

processes or voltage application in the molecular film might affect the conductance value 3) Noncovalent interaction between molecules in the molecular film can affect the conductance measurement 4) the conductance of the film per molecule might not be comparable with the conductance of a molecule obtained from the single molecule conductance measurement and last 5) the molecules in the films are not exposed to the outside world.

1.1.2 Single Molecule Measurement

In the single-molecule conductance measurement, first a single molecule must be reliably wired between electrodes with well-defined contact geometry, second the environmental conditions must be carefully controlled, and third a signature should be provided to identify if the measured conductance is representing only the single sample molecule conductance. When satisfying these conditions, there are three different methods to measure the conductance of a single molecule 1) scanning probe method, 2) fixed electrodes, and 3) a mechanically controlled molecular junction.

In the scanning probe method, Scanning Tunnelling Microscopy (STM) and Atomic Force Microscopy (AFM) are used for measuring the electric property of a single molecule adsorbed on a conductive substrate. In both types of microscopy, a tip place over the surface a determined distance away enable one to detect any individual molecule and measure its property. Both methods have had an important role in the field of molecular electronics. The tip-molecule contact is often the source of error in both types of microscopy for determining absolute conductance of the molecule.

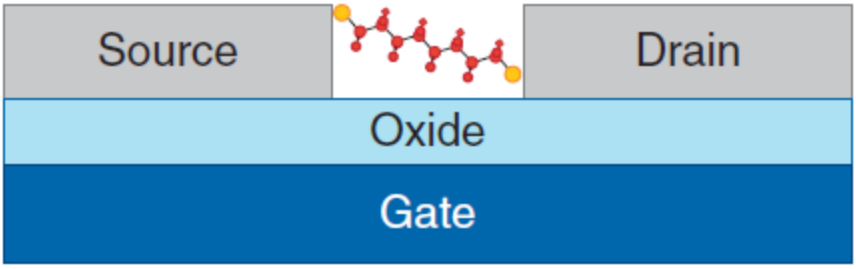

Figure 1.3: Experimental Set-up for Molecular Conductance Measurements with the Fixed Electrode Method (Chen et al., 2007).

In fixed electrode methods, two electrodes are fixed on a surface with a determined distance between them and the molecule of interest bridging the two electrodes (Figure 1.3). The difficult, and very important step of this experiment is fabricating electrodes with a molecule-scale gap. Since a vast majority of molecules are a few nanometers or less, usually the fabrication of such a small gap between electrodes is hard to reach by using conventional micro and nano-fabrication facilities. The difficulties of fixed electrode method are: 1) the fabrication process for fixing electrodes are not usually reproducible 2) it's difficult to put just one molecule between two electrodes 3) the interaction between molecules and electrodes is not well known and 4) the structure of the electrodes and the position of the molecule are not precisely known.

In mechanically controlled molecular junctions, one can control the gap between two electrodes with sub-angstroms precision by using a piezoelectric transducer (PZT) or other mechanical actuation mechanisms. Based on this method, it's possible to fabricate molecular junctions and measure the conductance of various molecules.

In general, the critical issues in all above mentioned methods are molecular-electrode

contact geometry, molecular-electrode energy level alignment, effect of external force, effect of environment, and current-induced local-heating effect.

1.2 Theoretical Framework to Compute Molecular Conductance

This part focuses on electron transport through molecular layers and single molecule between two regions of free or quasifree electrons. The primary important issue in this field is understanding the interrelationship between the molecular structure of such junctions and their transport properties. "Such investigations of electrical junctions, in which single molecules or small molecular assemblies operate as conductors connecting traditional electrical components such as metal or semiconductor contacts, constitute a major part of what has become the active field of molecular electronics" (Nitzan, 2001).

1.2.1 Modeling the Conductance of a Thin Molecular Layer

Let's consider a simple model for Metal-Insulator-Metal (MIM) junction represented by a continuum of electronic level for the right and left electrodes, with their Fermi levels displaced to include the effect of the applied bias (Simmons, 1963).. The insulator acts like a barrier and electron transport corresponds to a one-dimensional tunneling process through the barrier. Based on the Wentzel-Kramers-Brillouin (WKB) approximation, if a particle with mass of m and velocity v_x is scattered by a

rectangular barrier with height $U(x)$, the probability of transmission $\mathcal{T}(E)$ would be:

$$\mathcal{T}(E) = exp[\frac{-4\pi}{\hbar}\int_{s_1}^{s_2}[2m(U_B(x) - E_x)]^{1/2}\,dx] \tag{1.1}$$

s_1 and s_2 are the turning points for $U_B(x)$. The tunneling flux is obtained by: $\mathcal{T}(E_x)n(E_x)\sqrt{2E_x/m}$. $n(E_x)$ is the number of electrons per unit volume with the energy of E_x in x direction which can be obtained by integrating of Fermi-Dirac distribution equation with respect to E_y and E_z. Assuming that the right electrode is positively biased with respect to the left electrode (the two electrodes are identical), the net current which is dependent on transmission probability and probability of finding an electron with E_x per unit time unit volume is given by (Simmons, 1963):

$$J = \int_0^\infty \mathcal{T}(E_x)\xi(E_x)\,dE_x \tag{1.2}$$

where,

$$\begin{aligned}\xi(E_x) &= \frac{2m^2e}{(2\pi\hbar)^3}\int_{-\infty}^{\infty} dv_y \int_{-\infty}^{\infty}[f(E) - F(E - e\Phi)]\,dv_z \\ &= \frac{4\pi me}{(2\pi\hbar)^3}\int_0^\infty [f(E) - F(E - e\Phi)]\,dE_r\end{aligned} \tag{1.3}$$

Where $E_r = E - E_x = (1/2)m({v_y}^2 + {v_z}^2)$ is the sum of kinetic energy of the electron in y and z directions, and Φ is the bias voltage. At zero temperature and when $\Phi \to 0$, one can get $f(E) - F(E - e\Phi) = e\Phi\delta(E - E_F)$. Therefore Equations 1.2 and 1.3 lead to an expression giving conduction per unit area, i.e. conductivity per unit length:

$$\sigma_x = \frac{4\pi me^2}{(2\pi\hbar)^3}\int_0^{E_F} \mathcal{T}(E_X)\,dE_x \tag{1.4}$$

These equations have been successfully used for predicting the conductance and current-voltage characteristic of a very thin insulator film sandwiched between two metal electrodes at finite Φ. Simmons has derived the approximate form of these expression based on the dependence of Φ-drop along the insulator which will be discussed in detail later (Simmons, 1963). For deriving the equations above, we assumed that the conductance and tunneling current are only dependent on the kinetic energy of the electron in the x direction which in turn relies on our simple picture of the planar geometry of the electrodes as well as the explicit form of Equation 1.1. This assumption is not valid for a typical STM configuration that involves a tip on one side and a structured surface on the other. Tersoff and Hamman (Tersoff et al., 1985) have applied Bardeens formalism (Bardeen, 1961) to include the effects of the asymmetry of the electrodes in their calculations.

Equations 1.1-1.4 are the special case of a more general formalism of the current-voltage characteristic and the conduction of a given junction derived by Landauer (Landauer, 1970). In the Landauer formalism, we have a system comprised of two one-dimentional (1D) leads connected by a scattering object or a barrier characterized by a transmission function $\mathcal{T}(E)$. In this picture, conductance can be obtained by computing the total unidirectional current created in an ideal lead by electrons in the energy range of $[0,\hbar^2{k_E}^2/2m]$. For a one-dimensional (1D) ideal lead with length L, the density of the electron with the wave vector of k to $k+dk$ is $n(k)dk = 2(1/L)(L/2\pi)f(E_k)dk = f(E_k)dk/\pi$. The corresponding velocity of these electrons is

$v = \hbar k/m$. therefore based on the definition of current, we get:

$$J = e\int_0^{k_E} dkv(k)n(k) = e\int_0^{k_E} dk(\hbar k/m)f(E)/\pi = \frac{e}{\pi\hbar}\int_0^{E_k} dEf(E) \tag{1.5}$$

Using this equation, the net current under the bias can be obtained by:

$$J = \frac{e}{\pi\hbar}\int_0^{\infty} dE[f(E) - f(E - e\Phi)] \tag{1.6}$$

At zero temperature and at the limit of $\Phi \to 0$, the net current in an ideal lead, based on equation 1.6, is given by:

$$J = \frac{e^2}{\pi\hbar}\Phi \tag{1.7}$$

Therefore, the conductance of an 1D ideal lead would be $J/\Phi = e^2/\pi\hbar$ at zero temperature. In the presence of a scatterer, equation 1.6 is replaced by:

$$J = \frac{e}{\pi\hbar}\int_0^{\infty} dE[f(E) - f(E - e\Phi)]\mathcal{T}(E) \tag{1.8}$$

Where at zero temperature and close to zero bias, we get:

$$g = J/\Phi = \frac{e^2}{\pi\hbar}\mathcal{T}(E_F) \tag{1.9}$$

Equation 1.9 is only valid for a 1D lead. When the transmission takes place in the lead with finite sizes perpendicular to the propagation direction, equation 1.9 leads to (Imry, 1997):

$$g = \frac{e^2}{\pi\hbar}\sum_{i,j}\mathcal{T}_{ij}(E_F) = \frac{e^2}{\pi\hbar}\mathbf{Tr}(SS^{\dagger})_{E_F} \tag{1.10}$$

Where $\mathcal{T}_{ij} = |S|^2$ is the transmission probability of an electron coming from , say, the left side with the transversal mode of i and is scattered into the right side with

the transversal mode of j. In Equation 1.10, the sum is over all transversal mode associated with an energy lower than E_F. Let's consider a planar-tunnel junction when tunnelling transmission can take place in only one direction, the x direction. In this case, scattering does not couple too many different transversal modes and the transmission function would be only dependent on the energy of the electron in the x direction. Therefore, equation 1.10 leads to:

$$\begin{aligned}\sum_{i,j}\mathcal{T}_{ij}(E_F) &= \sum_{i,i}\mathcal{T}_{ii}(E_F) \\ &= \frac{L_y L_z}{2\pi^2}\int dk_y \int \mathcal{T}[E-(\hbar^2/2m)({k_y}^2+{k_z}^2]\,dk_z \\ &= \frac{L_y L_z}{2\pi^2}\frac{2\pi m}{\hbar^2}\int_0^E \mathcal{T}[E-E_r]\,dE_r\end{aligned} \tag{1.11}$$

$E_r$was defined earlier. Based on this equation, the conductivity per unit area would be:

$$\sigma \equiv \frac{g}{L_y L_z} = \frac{4\pi m e^2}{(2\pi\hbar)^3}\int_0^{E_F}\mathcal{T}(E_X)\,dE_x \tag{1.12}$$

Which is in agreement with Equation 1.4.

The transmission coefficient in the above equations can be replaced by the scattering amplitude or T matrix elements, between unperturbed states localized on the electrodes.

$$\sum_{i,j}\mathcal{T}_{ij}(E_F) = 4\pi^2\sum_{l,r}|T_{lr}|^2(E)\delta(E-E_l)\delta(E-E_r) \tag{1.13}$$

On the left side of equation 1.13, the states of i, l denotes the exact scattering states with energy E, characterized by an incoming state i on the left electrode and an outgoing state j on the right electrode. On the right side of the equation, l, r

denote zero order states localized on the right and left electrode, respectively. T is the related scattering (transition) operator whose particular form is dependent on the details of this localization. Using an expression similar to the Golden Rule for the scattering operator, we can write:

$$\begin{aligned} J &= \frac{4\pi e}{\hbar}\int_0^\infty dE[f(E)-f(E-e\Phi)]\sum_{l,r}|T_{lr}|^2(E)\delta(E-E_l)\delta(E-E_r) \\ &= \int_0^\infty dE[f(E)-f(E-e\Phi)]\frac{g(E)}{e} \end{aligned} \tag{1.14}$$

$$g(E) = \frac{4\pi e^2}{\hbar}\sum_{l,r}|T_{lr}|^2(E)\delta(E-E_l)\delta(E-E_r) \tag{1.15}$$

The most difficult part of the above equations is calculating the T matrix. Green function method is one of the most popular methods among the different methods that have been proposed for calculating the T matrix. This method will be explained later in more detail. When $\Phi \to 0$, Equation 1.14 leads to $J = g\Phi$ and the conductance would be:

$$g = g(E_F) \tag{1.16}$$

Equations 1.13-1.16 provide a complete model for calculating the conductance of a thin molecular layer.

1.2.2 Modeling the Conductance of a Single Molecule

Equations 1.14-1.16 provide a convenient starting point for most treatments of currents through a molecular junction where the direct coupling between two elec-

trodes is weak. In order to obtain the scattering operator, it is convenient to write the Hamiltonian of the system as the sum $H = H_0 + V$. H_0 represents the Hamiltonian of the isolated electrodes and molecular junction and V represents the coupling between them. In the case of weak coupling limit, scattering operator T is given by:

$$T(E) = V + VG(E)V; G(E) = (E - H + i\epsilon)^{-1} \tag{1.17}$$

The first term is related to the direct coupling between l and r states, representing states localized on left and right electrode respectively, which can be neglected in very weak direct coupling. The second term corresponds to indirect coupling between l and r via the molecular junction.

In the simple case, the molecular junction can be modeled as N localized sites in which only site 1 is coupled directly to left electrode and site N is coupled to right electrode. Using this assumption, we can write $T_{lr} = V_{l1} G_{1N} V_{Nr}$ and at zero temperature, based on this operator, transmission elements can be obtained by following equation(Mujica et al., 1994):

$$\sum_{i,j} \mathcal{T}_{ij}(E_F) = |G_{1N}(E_F)|^2 \Gamma_1^{(L)}(E_F) \Gamma_N^{(R)}(E_F) \tag{1.18}$$

Using Equations 1.14 and 1.15:

$$J(\Phi) = \frac{e}{\pi\hbar} \int_{E_F - e\Phi}^{E_F} dE |G_{1N}(E, \Phi)|^2 \Gamma_1^{(L)}(E) \Gamma_N^{(R)}(E + e\Phi) \tag{1.19}$$

Where G_{1N} is one element of the reduced Green's function in the bridge subspace, obtained by projecting out the electrodes states:

$$G(E) = (E - H_B - \Sigma_B(E))^{-1} \tag{1.20}$$

Here $H_B = H_B^0 + V_B$ is the unperturbed Hamiltonian of the molecular junction (bridge) and can be presented by:

$$H_B^0 = \sum_{n=1}^{N} E_n |n\rangle\langle n|; V_B = \sum_{n=1}^{N}\sum_{n'=1}^{N} V_{n,n'} |n\rangle\langle n'| \tag{1.21}$$

Also $\Sigma_B(E)$ is given by:

$$(\Sigma_B(E))_{n,n'} = \delta_{n,n'}(\delta_{n,1} + \delta_{n,N})(\Lambda_n(E) - i(1/2)\Gamma_n(E)) \tag{1.22}$$

$$\begin{aligned} \Gamma_n(E) &= \Gamma_n^{(L)}(E) + \Gamma_n^{(R)}(E) \\ &= 2\pi \sum_l |V_{ln}|^2 \delta(E_1 - E) + 2\pi \sum_r |V_{rn}|^2 \delta(E_N - E) \end{aligned} \tag{1.23}$$

$$\Lambda_n(E) = \frac{PP}{2\pi} \int_{-\infty}^{\infty} dE \frac{\Gamma_n(E')}{E - E'} \tag{1.24}$$

$\Sigma_B(E)$, $\Gamma_n(E)$, and $\Lambda_n(E)$ are the self-energy operator, its width, and its associated shift, respectively. Γ and Λ represent the life time of staying electron on the molecular junction. Since all these operators span the bridge subspace, they would be $N \times N$ matrixes. In the simple case of the tight binding model and in the weak coupling limit, G_{1N} leads to:

$$G_{1N} = \frac{V_{1,2}}{(E - E_1 - \Sigma_1(E))(E - E_N - \Sigma_N(E))} \prod_{j=2}^{N-1} \frac{V_{j,j+1}}{E - E_j} \tag{1.25}$$

Equations 1.18-1.25 provide a complete simple model to calculate the molecular conductance. One of the convenient methods to calculate the required parameters in the mentioned equations is the methods based on Density functional Theory (DFT). Therefore, some researchers have developed different DFT methodology to the problem of electron transport via atomic or molecular bridges. For instance, in Lang's

approach (Lang, 1995; Lang et al., 200; Parr et al., 1989), the single-electron wavefunction $\psi_0(r)$ and the electron density $n_0(r)$ for two bare metal (jellium) electrodes are computed based on DFT and these wavefunctions are used in the Lippman-Schwinger equation:

$$\psi(r) = \psi_0(r) + \int dr' dr'' G^0(r, r') \delta V(r', r'') \psi(r'') \tag{1.26}$$

to obtain the **single-electron** scattering wavefunction $\psi(r)$ in the presence of a molecular junction, where G^0 is the Green Function of the bare electrode and δV is the potential difference between bare electrodes and electrodes with the molecular junction. Equation 1.26 gives the scattering states labelling by their energy, the momentum in direction yz parallel to the electrodes $k_{||}$, the sign of the momentum in the x direction, and their spin. Close to zero temperature, current density based on the obtained scattering states would be:

$$J(r) = -2 \int_{u_L}^{u_R} dE \int d^2 K_{||} Im\{\psi_+^* \nabla \psi_-\} \tag{1.27}$$

The factor 2 accounts for the double occupancy of each orbital. This approach was used recently (Di Ventra et al., 2000) to calculate current through a molecular species, benzene 1,4-dithiolate molecule (as used in the experiment of Reed et al. 1997), between two jellium surfaces and has demonstrated the large sensitivity of the computed current to the microscopic structure of the molecule-metal contacts. However, one of the most important issues in the DFT methodology is that DFT is not able to fully describe the infinite and non-equilibrium system underlying electron transport process in the experimental set-up. Thus, another powerful formalism

has been developed based on non-equilibrium Green's Function that enable one to compute molecular conductance while considering the effect of the infinite size and non-equilibrium state of the system (Xue et al., 2002). This formalism will be explained briefly in the method and results sections.

1.3 The Relationship Between Molecular Conductance and Molecular Electronic Structure.

As seen in previous sections, studying molecular conductance is demanding and challenging work in both experimental and theoretical treatments. Therefore, finding a molecular descriptor for the conductance which is easy to measure and calculate is very desirable and interesting from a purely theoretical standpoint and also experimental view point for designing new junctions with tailored properties as building blocks in future generation nano-electronic devices (Gonzale et al., 2006; Mujica et al.,2000; Lafferentz et al., 2009; Galperin et al., 2008; Nitzan et al., 2003; Joachim et al., 2000; Tao, 2006). Unfortunately, despite the immense advances during the past decade in both theory and experiment, understanding, interpreting, and modelling the transport properties of a simple molecular junction based on the simple electronic properties, remains an important and desirable task.

Generally speaking, transport in a junction is a complex non-equilibrium problem where the description of the current should include, in principle, many-body and vibronic effects (Liu et al., 2014). In such a description, the conductance of the device, consisting of the molecule and the electrodes operating under a bias potential, cannot

be separated into a molecular and an electrode contribution and it depends, in a complicated way, on the nature and strength of the molecule-electrode coupling and the voltage (Hartle et al., 2009; Bergfield et al., 2009; Baer et al., 2003).

However, in the limit of low voltage, which physically corresponds to the linear response regime, it is possible to define a voltage-independent molecular conductance. This property is affected by both the nature of the anchoring groups connecting the molecule to the electrode and ,more importantly for our study, by some intrinsic properties of the molecule (Nitzan, 2006). For instance, it has been shown that the gap between HOMO and LUMO (E_g), molecular conformation and molecular bond characteristic have a determining role in the molecular conductance (Magoga et al., 1997; Xue et al., 2001; Tomfohr et al., 2002; Pauly et al., 2008; McDermott et al., 2009; Kamenetska et al., 2010; Burkle et al., 2012; Venkataraman et al., 2006).

In addition to the intrinsic electronic properties of the molecule, the conductance of a molecular junction also depends on the chemical nature of the anchoring groups, the position of the Fermi energy level of the electrode, and the contact geometry of the molecule and electrodes (Kiguchi et al., 2010; Park et al., 2007; Chen et al., 2006) named here as environmental factors. By assuming and keeping environmental factors consistent, we study the effect of the polarizibilty of a molecular junction biased by a finite potential on its conductance. The possible connection between molecular conductance and polarizability may be understood from the heart of theoretical framework which has been proposed for decades to model molecular conductance. As

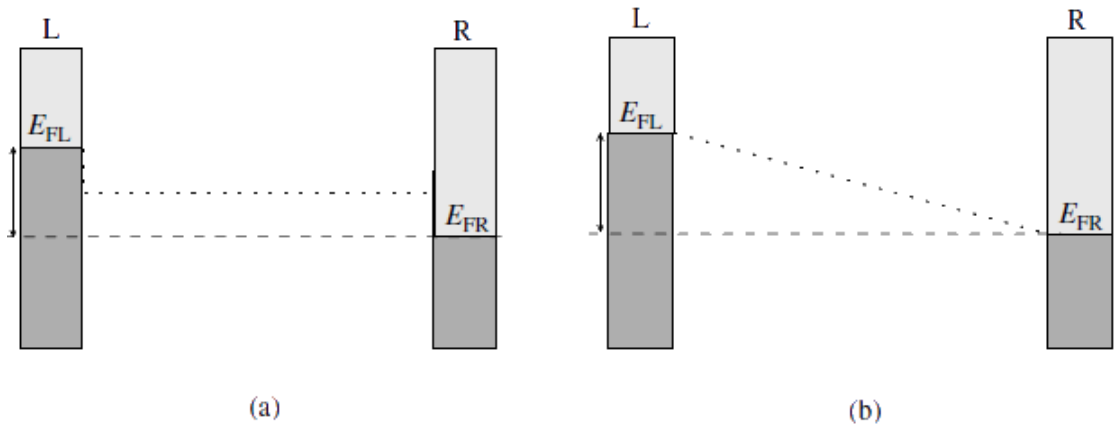

Figure 1.4: Spatial Profile Potential of an Electrode-Bridge-Electrode Structure with a (a) Very Easy Polarizable Medium (b) Unpolarizable Medium, as the Bridge (Nitzan, 2006).

described in a previous section, the conductance of a molecular junction depends on the transmission function, which in turn depends on the electrical potential biased on the molecular junction. Based on how this biased electrical potential drops along the molecular bridge, the transmission function and consequently the conductance would be different. As a matter fact, electrostatic potential dropping or spatial profile of the electrostatic potential is highly dependent on the polarizability of the junction. Figure 1.4 shows the schematic spatial profile potential for two extreme cases (Nitzan, 2006).

The physical plausibility of the connection between molecular conductance and polarizability becomes stronger based on the results of recent works in trying to describe the spatial profile of the electrostatic potential by solving in a self-consistent way Schrdinger and Poisson equations to connect the quantum electronic density to

the electrostatic potential (Gonzalez et al., 2006; Xue et al., 2001). This model reveals essential features of the interplay between the molecular charge density and the spatial profile of the field across the junction, a key variable in determining the rectification properties of the device (Metzger, 2003). The picture that emerges from this model is that molecules behave to a large extent as a dielectric whose polarization response counteracts the driving field. This leads to a spatial profile that differs substantially from that of a vacuum junction between two electrodes, which is a linear function of the inter-electrode separation as found by solving Poisson equation for zero charge density, and corresponds rather to an S-shaped function associated with a spatial profile characterized by the fact that the potential drop occurs at the interfaces between the molecule and the electrodes.

Once one has accepted the crucial role played by the molecular bridge in determining the local dielectric properties of a junction, the next conceptual step is to connect the dielectric constant to the molecular polarizability. It comes perhaps as a surprise that the validity of the age-old Clausius-Mossotti equation, that relates the static molecular polarizability of a simple dielectric material to its macroscopic dielectric constant, has been explored in the nano-domain and found to work reasonably well using a state-of-the-art description of the electronic structure of electrified interfaces (Natan et al., 2010; Bergren et al., 2010). In a way, this result is a consequence of the connection between Maxwell's equations of electromagnetism and quantum mechanics, which requires that the charge and the current densities be calculated via

the Schrödinger equation to obtain a consistent description.

One of the earliest models to explicitly connect electron transport to the dielectric properties of a junction is a generalized version of Simmons model of tunneling through a continuous barrier whose properties depend on the charge and dielectric properties of the junction. It has been previously established that under some approximations it is possible to map a molecular orbital description of a molecule into a tunneling barrier, in such a way that the barrier height and width correspond to the energy difference between the Fermi energy and the energy of the bridge molecular orbitals and the length of the molecule, respectively (Mujica et al., 2001). Inspired by the connection discussed above and earlier works that hinted to the importance of molecular polarizability (Bergren et al., 2010; InhetPanhuis et al., 2004; Munn et al., 2002), we decided to explore the consequences of using molecular polarizability to calculate the local dielectric constant in a tunneling model as well as the direct correlation between polarizability and the zero-voltage conductance calculated using a DFT-NEGF approach. The results of such a comparison are very encouraging and have led us to a more thorough theoretical investigation of the connection between the dynamic molecular polarizability and the ability of a molecule to transfer charge, either in the context of a molecular device or in an intra-molecular transfer process. The connection between polarizabilty and molecular conductance will be discussed with more details in a later section.

The rest of this thesis is organized as follows: Chapter 2 provides detailed informa-

tion on calculating the electronic structure, molecular conductance and polarizability. Chapter 3 provides a theoretical study as a proof of concept on the connection between polarizability and molecular conductance and also provides results with analysis of the data obtained by DFT calculations. Finally, Chapter 4 finalize the dissertation with a discussion about the nature of the correlation between molecular polarizability and conductance and speculations about future work.

Chapter 2

METHODS

In this chapter, a brief overview of the computational method used in this thesis is given. Part of this work is based on density functional theory (DFT) and the Non-Equilibrium Green's Function(NEGF). The electronic structure, conductance, and polarizability of a molecular system are described from first principles. In the first part of this chapter, an overview of the detail of the calculations will be given. In the second part, a brief overview of important aspects of DFT is given, as employed for the electronic structure calculations in this thesis. Also, the concepts of basis sets and pesudopotential functions will be briefly described. In the last part of the chapter, the NEGF for the description of the elastic current will be introduced.

2.1 Computational Details

Full geometry optimizations of all structures, including hydrogen-bonded complexes and the corresponding monomers were carried out at DFT-level as implemented in the ORCA 2.9 software package using the Becke gradient-corrected exchange functional and Lee-Yang-Parr correlation functional with three parameters (B3LYP) and the 6-311++G(2d,2p) basis set (Neese, 2012; Becke, 1993; Lee et al., 1988; Krishnan et al., 1980; Clark et al., 1983; Frisch et al., 1984; Curtiss et al., 1998; Hazra et al., 2012). This level of calculation was found to accurately describe the properties all studied systems in this work (Hazra et al., 2012; Rustad et al., 2010; Foreman et al.,

2003; Li et al., 2001). The calculated interaction energies were corrected for basis set superposition error using the Boys and Bernardi counterpoise correction (Boys et al., 1970). In the present work, the static dipole polarizability was partitioned into individual atomic components using a recent approach based on Hirshfeld population analysis $\alpha_{\gamma\gamma}$(Marenich et al., 2013). In this method, the spherically averaged molecular static dipole polarizability can be partitioned over all atoms i in a molecule as

$$\alpha_{\gamma\gamma} = \sum_i \alpha_{\gamma\gamma i} \tag{2.1}$$

using the following relation:

$$\alpha_{\gamma\gamma i} = \lim_{F_\gamma \to 0} \frac{\mu_{\gamma i}(F_\gamma) - \mu_{\gamma i}(0)}{F_\gamma} \tag{2.2}$$

$$\alpha = \frac{\sum_\gamma \alpha_{\gamma\gamma}}{3} \tag{2.3}$$

$$\begin{aligned} \alpha_{\gamma\gamma} &= (\frac{\partial \mu_\gamma}{\partial F_\gamma})_0 \\ &= \lim_{F_\gamma \to 0} \frac{\mu_\gamma(F_\gamma) - \mu_\gamma(0)}{F_\gamma} \end{aligned} \tag{2.4}$$

where μ_γ is the component of the dipole moment along the γ axis, with $\gamma = x, y,$ or z. F_γ is the magnitude of an auxiliary static electric field F used in the calculation, oriented along theγ axis, and 0 indicates $F = 0$. Averaging over α_{xx}, α_{yy}, and α_{zz} yields the spherically averaged molecular static dipole polarizability. Each component of the molecular polarizability tensor is then written is a sum of the individual atomic polarizabilities.

Since the major aim of the current investigation is to examine the nature of electronic transport across a hydrogen bond, the transport properties were obtained using the ab initio program TRANSIESTA (Soler, et al., 2002). The program uses the Hamiltonian provided by the DFT code SIESTA (Soler, et al., 2002), in combination with the nonequilibrium Greens Function formalism (Datta, 2000; Ferry et al., 2009; Landauer, 1957; Bttiker, 1986). Norm-conserving pseudopotentials account for the core electrons and a linear combination of pseudoatomic orbitals span the valence states. The calculations used a single-ζ basis set for the all the atoms and an energy cutoff of 300 Ry was chosen to define the real-space grid. The local density approximation (LDA) was employed to account for exchange and correlation effects (Perdew et al., 1981). 30 points of contour integration on the imaginary plane is used to obtain the density matrix from the Greens Function. A cut off energy of 380 Ry for the grid mesh is employed to have converged transmission values at zero bias. The molecular condutance was obtained by multiplying the calculated transmission values with the value for quantum conductance ($7.75 \times 10^5 S$) (Zimbovskaya et al., 2011).

Prior to evaluation of the transport properties, gold electrodes were attached to either side of the structure through a sulfur atom. Earlier local density approximation (LDA) calculations indicated that the C-S bond length was 1.76 $\mathring{A}$ in the energetically most stable conformation of molecules attached to gold atoms (Maniu et al., 2007). LDA calculations of dithiol-terminated oligo(phenylene-ethynylene)-type molecules attached to two gold electrodes indicated that the sulfur atom bound to the hollow-

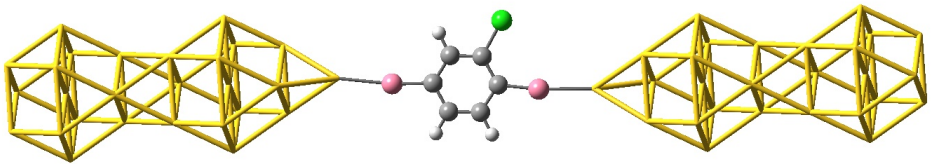

Figure 2.1: A Typical System Set-up in this Study Comprised of Gold Electrode, Sulfur, Molecular Bridge, Sulfur and Gold Electrode.

site with a Au-S distance of 2.4 $\mathring{A}$ was found to be energetically most stable (Kaliginedi et al., 2012; Haiss et al., 2006; Martin et al., 2010). In all our transport calculations, the structures were attached to the gold through the hollow-site with a S-C distance of 1.76 $\mathring{A}$ and a Au-S distance of 2.4 $\mathring{A}$. A schematic of the (Au electrode)-H-bonded complex-(Au electrode) model used to calculate the conductances reported in this work is shown in Figure 2.1.

Some of the important concepts and aspects of DFT and Green's Function used in ORCA 2.9 and SIESTA will be briefly explained below, a full description of the codes are available in Refs. (Soler et al., 2002; Artacho et al., 2008) (SIESTA), Refs. (Neese, 2012) (Abinit) and references therein.

2.2 Density Functional Theory

DFT is a theory in quantum mechanics used in physics, chemistry, and material science as an alternative to solving the many-body wavefunction associated with Schrödinger equation. The demonstration of its validity is well-established for the ground state, and some theoretical issues remain open regarding its applicability to

excited states. The use of DFT in solving complicated many-body problem has led to a dramatic reduction in computational expense and time. this explains why DFT has become one of the most popular computational methods in computational chemistry.

DFT relies on Hohenberg-Kohn theorems which state (Hohenberg et al., 1964; Kohn et al., 1965):

Theorem 1. "If two systems of electrons have the same ground state density $\rho(r)$ while one is trapped in the potential $V(r)$ and the other in potential $V'(r)$ then,"

$$V(r) - V'(r) = Constant \tag{2.5}$$

From this theorem, one can conclude that $V(r)$ is a unique functional of ρ and consequently the obtained wave-function from the Schrödinger equation based on the given $v(r)$ would be also a unique function of ρ. Therefore, it is possible to define an energy functional as below:

$$E[\rho(r)] = F[\rho(r)] + \int_{-\infty}^{\infty} V(r)\rho(r)dr \tag{2.6}$$

Based on this equation, one can prove that:

Theorem 2. "The global minimum of the energy functional, Equation 2.6, is the true ground-state energy, E_0, for the system and the density that minimizes the functional is the ground-state density, $\rho_0(r)$."

In Equation 2.6, $F[\rho(r)]$ is an universal functional containing the kinetic energy of electrons and the potential energy of the electrons resulting from the coulomb repulsion between them. In the majority of systems, $F[\rho(r)]$ is an extremely complicated functional whose exact form is not known, and should be approximated in some way. Despite the need for an approximate form of this functional, Hohenberg-Kohn

theorems still makes quantum mechanics calculations much simpler by mapping the many-body problem to an electron density problem dependent on just three spatial variables.

One of the earliest approximations for the universal functional, $E[\rho]$ was proposed by Kohn and Sham based on an effective potential model (Kohn et al., 1965). They introduced the idea of an auxiliary system of non-interacting electrons for which the kinetic energy functional and the exact density could be written in terms of one-electron Kohn-Sham orbitals. Employing this approximation, the many-body problem can be mapped into a set of coupled one-electron equations similar in spirit to the Hartree-Fock scheme but actually preserving the many-body character of the problem :

$$H\Phi_j(r) = \varepsilon_j \Phi_j(r) \tag{2.7}$$

$\Phi_j(r)$ is Kohn-Sham (KS)-wavefunction and ε_j is the eigenvalue of KS-wavefunction. The Hamiltonian of the system in Kohn-Sham formalism is:

$$H = -\frac{\bigtriangledown^2}{2} + V_{eff}(r) \tag{2.8}$$

and

$$V_{eff}(r) = V_{ext} + \int \frac{\rho(r')}{|r - r'|} dr + \frac{\partial E_{xc}[\rho(r)]}{\partial \rho(r)} \tag{2.9}$$

As seen, the effective potential includes three terms. The first term is the external potential described by the interaction between the nucleus (ion cores) and electrons (valence electrons), the second term is the repulsive coulomb interaction between electrons, and the third term is the exchange correlation energy, which is the most

complicated term and needs to be approximated. KS-equation should be solved iteratively as follows:

1) The initial form of $\rho(r)$ is guessed.

2) The KS Hamiltonian is constructed based on Equation 2.8.

3) The KS-orbitals are obtained via Equation 2.7.

4) The new electron density is calculated through $\rho(r) = \sum_j |\phi_j(r)|^2$.

5) If the difference between new and old electron densities is equal or lower to the convergence criteria, a solution to KS equations are is achieved otherwise the process is iterated from Step 2.

In solving KS equations, it is necessary to find an approximation for the exchange-correlation (XC) energy functional. The role of this functional in KS equation is to correct the error resulting from using the non-interacting kinetic energy of the electrons. Quantum treatment of electron-electron interaction includes Fermi correlation which prevents two electrons with parallel spins to be in the same point of space, coulomb correlation which describes the correlation between the position of two electrons due to the coulomb repulsion, and the correlation related to the overall symmetry of the system wavefunction. The exact form of XC functional is unknown, but there are some approaches to approximate this functional. The earliest approximation of XC functional was proposed by Kohn-Sham (Kohn et al., 1965) known as Local Density Approximation (LDA). E_{xc} obtained from LDA is described as follow:

$$E_{xc}^{LDA}(\rho) = \int \rho(r)\varepsilon_{xc}[\rho(r)]dr \tag{2.10}$$

Here ε_{xc} is the E_{xc} per electron in an homogenous electron gas. Since LDA gives a bad approximation of E_{xc} in some systems, there have been so many efforts to introducing a better functional for estimating E_{xc}. Maybe the best known functional for exchange-correlation energy after LDA is Generalized Gradient Approximation (GGA), which states that XC energy not only depends on the value of electron density but also depends on its spatial gradient (Perdew et al., 1992). The typical form for a GGA functional is;

$$E_{xc}^{GGA}(\rho) = \int \rho(r)\varepsilon_{xc}[\rho(r), \bigtriangledown\rho(r)]dr \tag{2.11}$$

GGA significantly improves on the LDAs description of the binding energy of molecules. This improvement caused the wide spread acceptance of DFT in the chemistry community in the early 1990s. It's worth mentioning that both E_{xc}^{LDA} and E_{xc}^{GGA} can be separated into two exchange and correlation parts (Harrison, 2003):

$$E_{xc}^{LDA}(\rho) = E_{x}^{LDA}(\rho) + E_{c}^{LDA}(\rho) \tag{2.12}$$

$$E_{xc}^{GGA}(\rho) = E_{x}^{GGA}(\rho) + E_{c}^{GGA}(\rho) \tag{2.13}$$

Based on this separation, different hybrid exchange correlation functionals have been proposed for further accuracy such as the linear combination of E_{xc}^{LDA} and E_{xc}^{GGA}. One of the well-known and successful hybrid functionals is B3LYP (Becke, three-parameter, Lee-Yang-Parr). This functional is defined as follows:

$$E_{xc}^{B3LYP} = E_{x}^{LDA} + a_0(E_{x}^{HF} - E_{x}^{LDA}) + a_x(E_{x}^{GGA} - E_{x}^{LDA}) + E_{c}^{LDA} + a_c(E_{c}^{GGA} - E_{c}^{LDA}) \tag{2.14}$$

Where E_{x}^{HF} is the HartreeFock exact exchange functional:

$$E_{x}^{HF} = -\frac{1}{2}\sum_{i,j}\int\int \psi_i^*(r_1)\psi_j^*(r_1)\frac{1}{r_{12}}\psi_i(r_2)\psi_j(r_2)dr_1dr_2 \tag{2.15}$$

The exchange-correlation functional used in this study was B3LYP.

2.3 Basis Sets and Pseudopotentials

As mentioned before, in order to solve the Kohn-Sham equation, an initial guess for $\rho(r)$ as the starting point of the calculations is required. The initial ρ can be obtained from the initial guess of a wavefunction constructed from a single Slater determinant of the orbitals that are generally expressed based on the linear combination of atomic wavefunctions of the atoms in the given system. Several different approaches have been proposed to generate atomic wavefunctions in order to correctly describe the behavior of the electrons in core and valance levels. These atomic wavefunctions are called basis sets. Four of the most popular basis sets are: Plane Waves, Gaussian, Augmented, and Numerical. Since I used Guassian type basis set in ORCA program, I will briefly explain this type of basis sets.

The basis set used in ORCA calculations for this study was $6-311^{++}G^{**}$. This basis set has been fully explained in several previous works (Ditchfield et al., 1971; Hehre et al., 1972; Hariharan et al., 1973; Hariharan et al., 1973), so here I present a brief summary of its properties. The 6 in the notation ($6-311^{++}G^{**}$) indicates that the program uses 6 primitive functions to construct a basis function/core orbital. The 311 in the notation means the program uses 3 valance basis functions/orbitals in which the first function has 3 primitives, the second one has 1 primitive, and the third one has also one primitive. The "++" in the notation means the program also uses diffuse functions for building the basis sets. The G in the notation means the program uses Gaussian type primitive to build basis functions. The "$**$" in the

notation means all heavy atoms get an extra d-function and all hydrogen atoms get an extra p-function. An example of a basis function with three parameters, is given as:

$$\phi_{1S}(r) = \Sigma_{i=1}^{3} a_i (\frac{2a_i}{\pi})^{3/4} e^{-\alpha_i r^2} \tag{2.16}$$

In this equation, the function $e^{-\alpha_i r^2}$ is called the primitive function (primitives). The coefficients a_i and α_i are optimized in a way so that the behaviour of the electrons (here core electrons) can be described accurately. In my calculations, I used triple-zeta basis sets for describing the valence electrons and minimal basis sets for describing core electrons. The triple-zeta basis sets is consists of three basis function with different number of primitives and minimal basis sets consists of just one basis function for each atomic core orbital. It is also possible to represent the core electrons and nucleus of an atom together with an effective potential or pseudopotential, while the electrons in the valence states are represented more explicitly (Troullier et al., 1991). Using this approach makes DFT calculations inexpensive and faster for systems containing many atoms and heavy atoms. There has been much effort in finding a way to create proper pseudopotentials, which are both successful in describing the all-electron behaviour correctly, and computationally efficient at the same time. In the SIESTA calculations performed in this study, the psuedopotential are created from all-electron atomic calculation performed in DFT through solving radial Kohn- Sham equations.

$$(-\frac{1}{2}\frac{d^2}{d^2 r} + \frac{l(l+1)}{2r^2} + v[\rho; r)])rR_{n,l}(r) = \varepsilon_{nl} rR_{n,l}(r) \tag{2.17}$$

Here $v[(\rho; r)]$ is the self-consistent one-electron potential:

$$v[\rho; r] = -\frac{Z}{r} + v_H[\rho; r] + v_{xc}[\rho(r)] \tag{2.18}$$

v_H is the Hartree potential, v_{xc} is the exchange-correlation potential functional of the core electrons, and $\rho(r)$ is the total electron density of the occupied orbitals by the core electrons. The psuedopotential should satisfy following conditions:

1) The pseudo-orbitals obtained from pseudopotential shouldn't have a node.

2) The normalized atomic radial pseudo-orbitals (PP), with angular momentum l, should be equal to the normalized radial all-electron orbitals (AE) after a given cutoff radius r_c

$$R_l^{PP}(r) = R_l^{AE}(r) \qquad for \qquad r > r_c \tag{2.19}$$

3) Both orbitals (PP and AE) should have the same charge inside of the cutoff radius as follow:

$$\int_0^{r_c} |R_l^{PP}(r)|^2 r^2 dr = \int_0^{r_c} |R_l^{AE}(r)|^2 r^2 dr \tag{2.20}$$

4) The eigenvalues of AE and PP orbitals must be the same.

The pseudopotentials with these conditions are usually called, "norm-conserving pseudopotentials". This type of pseudopotentials are used, by default, in both SIESTA and TRANSIESTA calculations.

Despite the core electrons, the valence electrons behaviour should still be described with a basis set composed of a linear combination of localized numerical atomic

orbitals (LCAO). In fact, the atomic orbitals are the product of a spherical harmonic and a radial function:

$$\Psi_{n,l,m}(r,\theta,\varphi) = R_{n,l}(r)Y_{l,m}(\theta,\varphi) \tag{2.21}$$

where $R_{n,l}$ and $Y_{l,m}$ are the radial functions with the principal quantum number of n and the real spherical harmonic for orbital angular momentum l and magnetic quantum number m, respectively. Since there is much freedom in how to combine atomic orbitals for building basis sets, the size and shape of the basis set is flexible. This flexibility can come from the number of angular momentum channels, the number of radial functions, the shape of radial function, and the cut-off radius. This includes the center (not necessarily atom centered), how many angular momentum channels around each centre, how many radial functions per angular momentum channel and last, the cut-off, r_c, and shape for each radial function. These parameters must be selected with care to maximize efficiency and accuracy. There are different ways to variationally generate optimized basis sets (Junquera et al., 2001), but there is still no well-defined way to generate the optimal basis set and check for convergence. In SIESTA, these optimal basis sets change from basis sets of single-ζ (SZ) type to multiple ζ including polarization and diffuse orbitals which can lead from fast and low convergence calculations to highly converged and more time consuming calculations. SZ is the minimal basis set which contains of one radial function per angular momentum channel. In this minimal basis sets, the number of angular functions are chosen based on the population of the electrons in the valence states of an given isolated

atom. In order to make the more flexible radial part, one more radial function can be added to generate a double-ζ (DZ) basis set. It is also possible to extend radial functions more and getting a multiple ζ basis.

2.4 Non-equilibrium Green's Function

The calculation of transport properties involves going beyond the description of the electronic structure and requires the consideration of non-equilibrium processes associated with the voltage bias. We are interested in the simplest molecular junction consisting of a molecule chemically connected to two electrodes. In such a system electrons are driven by the voltage bias and the description of the current requires, in principle, a many-body description. However, under some approximations a combination of DFT and transport theory has been implemented in several computational packages like TRANSIESTA. The quantum theory of transport is a complex subject that I will not attempt to treat here in any detail. For the purposes of this dissertation I will give only the basic equations involved in the calculation of the current and the conductance.

In general terms, the system is split into the electrode part where thermalization is assumed to occur and a bridge part where electrons are scattered. In Landauer's view of quantum transport it is precisely this scattering that is associate to the current. Transport itself is described in terms of a time-dependent propagator whose Fourier transform gives information about the stationary current, which is the main object of

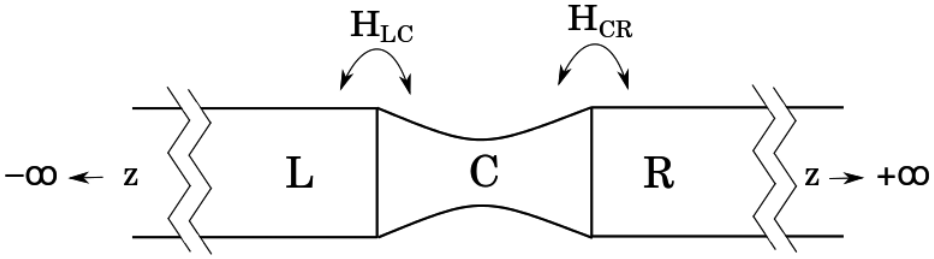

Figure 2.2: A Typical Scattering Region in Conductance Calculations (Löfås, 2013).

the DFT-NEGF approach. A schematic of the system considered in NEGF formalism is given in Fig. 2.2.

The electronic Hamiltonian of the above described system and its overlap matrix can be written as:

$$H = \begin{bmatrix} H_L & H_{LM} & 0 \\ H_{ML} & H_M & H_{MR} \\ 0 & H_{RM} & H_R \end{bmatrix}$$

$$S = \begin{bmatrix} S_L & S_{LM} & 0 \\ S_{ML} & S_M & S_{MR} \\ 0 & S_{RM} & S_R \end{bmatrix}$$

respectively. Let's assume that the Hamiltonian of the bulk in the L- and R-region can be converged. Therefore, we only need to compute the Hamiltonian and overlap matrix of M, M-L, and M-R. Based on this Hamiltonians, the transport properties of the molecule can be obtained by the finite L-M-R region of the infinite system, through a series of Green's Function matrices. When defining the retarded electronic single-particle Green's function $G^r(\varepsilon)$ as the inverse of $[(\varepsilon + i\eta)S - H]$, one can approximate

the description of the infinite system by considering the finite system L-M-R. For the molecular region (M), the retarded Green's Function can be written as follow:

$$G_M^r(\varepsilon) = [(\varepsilon + i\eta)S_M - H_M - \Sigma_L^r(\varepsilon) - \Sigma_R^r(\varepsilon)]^{-1} \tag{2.22}$$

Where ε is the energy of the electron, η is 0^+, and Σ_L^r and Σ_R^r are the self-energies operators for the left and right lead, respectively, due to the coupling between the molecule and the leads. The self-energy operator for the left electrode can be described as:

$$\Sigma_L^r(\varepsilon) = (H_{ML} - \varepsilon S_{ML}) g_L^r(\varepsilon) (H_{ML} - \varepsilon S_{ML}) \tag{2.23}$$

Where g_L^r is the retarded surface Green's function of the left electrode which described by $(\varepsilon S_L - H_L + i\eta)^{-1}$. Similarly self-energy operator can be also defined for the right electrode.

The current in this framework is given by (Xue et al., 2002):

$$J = \frac{ie}{2h} \int_{\mu_L}^{\mu_R} d\varepsilon \ (tr\{[f_L(\varepsilon)\Gamma^L - f_R(\varepsilon)\Gamma^R](G_M^r - G_M^a)\} + tr\{(\Gamma^L - \Gamma^R)G^<\}) \tag{2.24}$$

where μ_L and μ_R are the electrochemical potentials of the right and left electrodes that include the bias voltage (Meir et al., 1992; Jauho et al., 1994). All G functions in above and following equations are functions of the energy of the electron. Here $G^r, G^a, G^<$ stand for the retarded, advanced Green's function and "lesser" Keldysh function. The retarded Green function is related to the advanced Green function with the relation of $[G^r(\varepsilon)]^\dagger = G^a(-\varepsilon)$ (Di Ventra, 2008). $f_L(\varepsilon), f_R(\varepsilon)$ are the Fermi-Dirac distribution functions for the left and right electrodes, while Γ^L, Γ^R represent the

imaginary part of the self-energy. The lesser Keldysh function is related to the lesser self-energy by

$$G^{<} = G^{r}\Sigma^{<}G^{a}, \qquad \Sigma^{<} = i[\Gamma^{L}f_{L} + \Gamma^{R}f_{R}]. \tag{2.25}$$

Inserting Eq.(2.25) into Eq.(2.24), we have the more compact form for the current (Meir et al., 1992),

$$J = \frac{e}{h}\int_{\mu_L}^{\mu_R} d\varepsilon[f_L(\varepsilon) - f_R(\varepsilon)]tr[G^{a}\Gamma^{R}G^{r}\Gamma^{L}] \tag{2.26}$$

and the conductance is defined as,

$$g(E) = g_o tr[G^{a}\Gamma^{R}G^{r}\Gamma^{L}] = g_0 tr(\Gamma^{L}G^{r}_{M}\Gamma^{R}G^{a}_{M}) \tag{2.27}$$

Here g_0 is the quantum of conductance. In principle, the NEGF theoretical framework permits the description of elastic and inelastic transport (including electron-electron and electron-phonon interaction) through an appropriate inclusion of self-energies for each type of interaction (Galperin et al., 2007; Pleutin et al., 2003). It is however important to consider approximate schemes and the combination of non-equilibrium Green's function method with density functional theory have been extensively used for the approximate description of electron transport in molecular junctions.

Chapter 3

RESULTED AND DISCUSSION

This chapter is organized as follows. First we discuss the relevance of the local dielectric properties of the junction for transport based on NEGF formalism. Second, we discuss our results for the tunnelling model and different molecular systems, including two cases where both the polarizability and the conductance are calculated, and two cases where the conductance has been measured experimentally by other groups and the polarizability is calculated by us. Next, we extend our exploration to hydrogen bonded systems and some simple biological systems to check the validity of our correlation. We end with a discussion about the nature of this correlation between molecular polarizability and conductance and speculations about future work.

3.1 Model

3.1.1 Local Dielectric Constant and Voltage Profile

The conductance depends on the spatial profile of the electrostatic potential, which in principle has to be determined self-consistently through the simultaneous solution of the Schrödinger equation to calculate the charge density $\rho(\vec{r})$ and the Poisson equation to determine the electrostatic potential $\Phi(\vec{r})$. This is expressed schematically

as the following set of equations.

$$\begin{cases} H\Psi = E\Psi \\ \Psi \rightarrow \rho \\ \nabla^2\Phi = -\frac{\rho}{\epsilon_r} \end{cases} \tag{3.1}$$

Where ϵ_r is the dielectric constant of the inter-electrode medium. In a previous publication, Mujica et al. have used the scheme described by the set of Equations 3.1, for a one dimensional tight-binding system, and found that the self-consistent charge distribution for a finite applied voltage corresponded essentially to that of a polarizable dielectric. Similar conclusions using three-dimensional models and *ab initio* electronic structure methods have been found by Xue et al (Xue et al., 2001). These results strongly hinted at the importance of explicitly including the molecular polarization in a conductance model based on NEGF formalism combined with DFT. Driving our relation between conductance and molecular polarizability based NEGF goes through a barrier model of conductance which will be discussed in next sections. Before discussing about the barrier model of the conductance, the Clausius-Mossotti relation will be briefly explained because this relation is used in our barrier model.

3.1.2 Clausius-Mossotti Relation

The most straightforward connection between the dielectric constant ϵ_r of an electrified interface and the molecular polarizability α of the intervening medium is

given by Clausius-Mossotti equation:

$$\epsilon_r = \frac{\epsilon_0 + 2\gamma\alpha}{\epsilon_0 - \gamma\alpha}$$
$$\gamma = \frac{N_A d}{3M} \tag{3.2}$$

Where, N_A is the Avogadro's number, ϵ_0 is the vacuum permittivity, M is the molar mass of the material and d is its density. It applies to the dielectric constant of a bulk dielectric material that is homogeneous and isotropic, and it connects the static polarizability of a single molecule with the susceptibility of a three-dimensional molecular material. The basic microscopic premise of this relation is that in a uniform electric field, each molecule is represented as a polarizable point dipole that experiences the external field (thus inducing a polarization response). These conditions might seem too simplistic to describe a molecular junction, but the nanoscopic validity of the Clausius-Mossotti equation has been systematically explored (Natan et al., 2010) and it corresponds to a well-defined limit that provides us with a physically reasonable starting point.

3.1.3 Barrier Model of Conductance

To initially explore the connection between polarizability and conductance we consider a model of molecular conductance as a tunnelling process. This amounts to ignoring all the many-body aspects of the transport process, and assuming that the molecule acts as a one-dimensional tunnelling barrier, specified by two parameters: the height and the width. Simmons model, including image charges and dielectric effects, has been extensively used for the description of tunnelling through metal-

molecule interfaces with remarkable success (Simmons et al., 1963). We are particularly interested in the expression for the height of the tunnelling barrier, which has been shown in the Simmons model to be related to the dielectric constant by:

$$\bar{\phi} = \phi_0 - qV\frac{s_1 + s_2}{2x} - \frac{1.15\lambda x ln(\frac{s_2(x-s_1)}{s_1(x-s_2)})}{\Delta s} \tag{3.3}$$

with λ defined as:

$$\lambda = \frac{q^2 ln2}{8\pi x \epsilon_0 \epsilon_r} \tag{3.4}$$

Where, q is the electron charge, V is the bias voltage, ϕ_0 is the bare barrier height, s_1 and s_2 are the distances between the barrier and the two electrodes, $\Delta s = s_2 - s_1$, x is the midpoint between the electrodes, ϵ_0 is the vacuum permittivity and ϵ_r is the dielectric constant.

The relationship between the current and the voltage in the tunnel junction can be recast in a following form:

$$\begin{aligned} J &= c(\bar{\phi}e^{-A\sqrt{\bar{\phi}}} - (\bar{\phi} + qV)e^{-A\sqrt{\bar{\phi}+qV}}) \\ c &= \tfrac{q}{2\pi h(\sigma\Delta s)^2} \\ A &= (\tfrac{4\pi\Delta s}{h}\sqrt{2m_e}) \end{aligned} \tag{3.5}$$

Where σ is a correction factor defined in Ref (Simmons, 1963). The combined use of Eqs. 3.2 and 3.3 results in the desired connection between the effective barrier's height and the polarizability:

$$\bar{\phi} = \phi_0 - qV\frac{s_1 + s_2}{2x} - \frac{0.0317q^2 x ln(\frac{s_2(x-s_1)}{s_1(x-s_2)})}{(\Delta s)\epsilon_0}(\frac{\epsilon_0 - \gamma\alpha}{\epsilon_0 + 2\gamma\alpha}) \tag{3.6}$$

The differential conductance g is defined as

$$g(V) = \frac{\partial J}{\partial V} \tag{3.7}$$

The differential conductance in the limit of zero voltage can be obtained straightforwardly from Eq.(3.5) as:

$$\lim_{V\to 0} g(V) = qce^{-A\sqrt{\bar{\phi}}}\left(\frac{A\bar{\phi}}{2\sqrt{\bar{\phi}}} - 1\right) \tag{3.8}$$

In deriving Eq. 13, we assume that $\frac{s_1+s_2}{2x} = 1$ and that the molecular polarizability is not dependent on the bias voltage.

A different theory, based directly on the Green's function approach to transport, showing the explicit mapping of a one-dimensional tight-binding model of a molecule into a tunnelling barrier, was obtained by Mujica et al (Mujica et al., 2001). In this description, for a chain of N sites, characterized for an inter-site separation a, and a hopping integral t, the zero-voltage conductance is obtained as:

$$\begin{aligned} g &= g_0 e^{-\beta L} \\ g_0 &= \tfrac{2e^2}{\hbar}\tfrac{\Delta_0^2}{t^2} \\ \beta &= -\tfrac{2}{a} ln(\tfrac{t}{E_o}) \end{aligned} \tag{3.9}$$

Where E_o is the site energy with respect to Fermi energy level, $L = Na$ is the length of the chain, a is the inter-site distance and Δ_0 is the spectral density, equal to the $\Gamma_{R/L}$ in Eq.(2.24). Starting from Eq.(3.9) and replacing the parameter E_0 by the barrier height given by Eq.(3.6), $\bar{\phi}$ we obtain:

$$g = \frac{2e^2}{\hbar}\frac{\Delta_0^2}{t^2}\left(\frac{t}{\phi_0 - \frac{0.0317q^2 x ln(\frac{s_2(x-s_1)}{s_1(x-s_2)})}{(\Delta s)\epsilon_0}(\frac{\epsilon_0-\gamma\alpha}{\epsilon_0+2\gamma\alpha})}\right)^{2N} \tag{3.10}$$

Figure 3.1 shows a plot of conductance vs polarizability using both Simmon's continuous model of the barrier and Mujica's model based on a discrete site description.

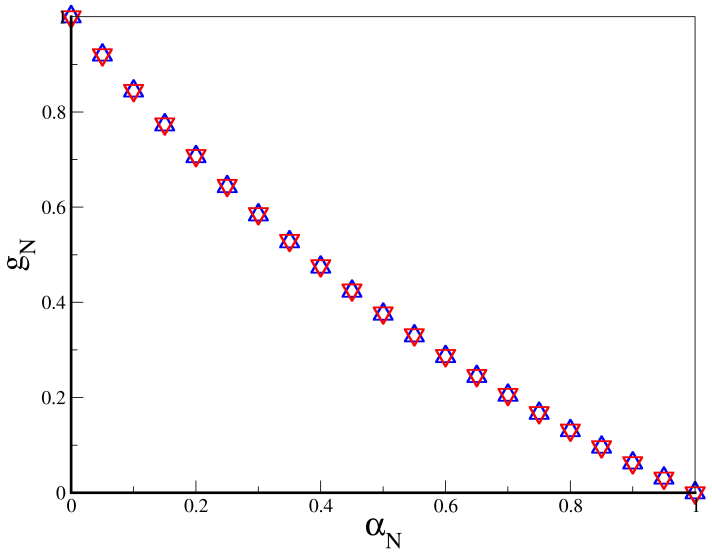

Figure 3.1: The Predicted Trend Between Conductance and Polarizability Based on Eq.(3.5) and Eq.(3.10). The Blue Upward Triangle Represent Normalized Conductance Values That Are Calculated Using Eq.(3.5) and Red Downward Triangle Are Based on Eq.(3.10). Both Approaches Predict Identical Behaviour for Conductance vs Polarizability.

We use normalized values of these quantities, defined by $X_N = \frac{X - X_{min}}{X_{max} - X_{min}}$, to eliminate irrelevant dependencies on the parameters for each model. It is apparent that in both cases the physical intuition based on the dielectric description of the junction is borne out by the calculations and that the agreement between the two models is nearly perfect and thus gives us a more precise picture of the connection between conductance and polarizability. A thorough comparison between the predictions of these two models, for instance for the length dependence, can be found elsewhere (Mujica et al., 2001).

3.2 Molecular Models

Given the encouraging results obtained with the tunnelling description, we decided to test our idea with more realistic molecular models, where in all cases we have used as a measure of the molecular property the isotropic polarizability, $\bar{\alpha}$ defined in terms of the polarizability tensor as $\bar{\alpha} = (1/3)tr(\alpha)$ (Martin et al., 1979). The computational details can be found in the method section.

We first calculated conductance and polarizabilities of a series of π conjugated aliphatic chains with different lengths obtained by adding C_2H_4 units. This effect has been studied experimentally and theoretically in similar systems (Tao, 2006; Li et al., 2006; Engel et al., 2004; Liu et al., 2008) and the STM current shows an exponential decay with increasing length, a result fully consistent with the idea that under some conditions the bridge molecule in a STM junction behaves essentially as a tunneling barrier. More interestingly is the fact that for families of related molecules, the static isotropic polarizability scales with the molecular volume (Ratkova et al., 2011) We then have two equations giving the conductance and the polarizability as an approximate function of molecular length:

$$g = Ae^{-\beta L} \tag{3.11}$$

$$\bar{\alpha} = BL^3 \tag{3.12}$$

where A, B and β are constants characteristic of the molecular system and the molecular volume has been simply approximated as scaling as L^3. The implication of these

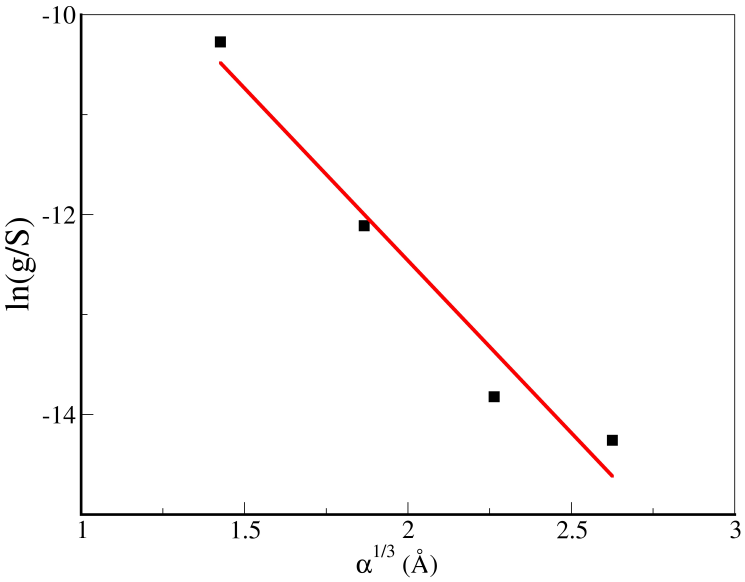

Figure 3.2: Calculated Conductance Versus Calculated Polarizability for π-Conjugated Chains. As Seen, the Predicted Trend Is Observed for These Chains. The Points on the Graph Correspond to C_2H_4 to C_8H_{18}. The Correlation Coefficient R^2 for the Fitting Line Is 0.9606 and the Equation of the Fitting Line Is $ln(g) = -3.4474\alpha - 5.5639$.

equations is that the conductance should be related to the polarizability simply as

$$g = Ce^{-\beta'\tilde{\alpha}^{1/3}} \tag{3.13}$$

where the new constants C and β' can be obtained straightforwardly from those in equations 3.11 and 3.13. The linear relationship between the log of g and the the third root of the polarizability is clearly displayed in Figure 3.2, confirming the validity of Eq.(3.13). We next put our model to another test, where we examined the correlation between polarizability and conductance for a benzene ring with different substituents

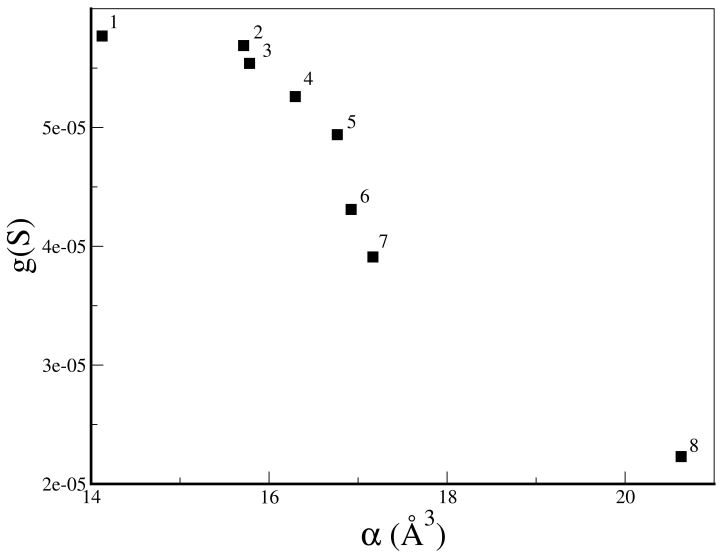

Figure 3.3: Calculated Conductance Versus Polarizability for Different Substituted Benzene Rings. As Seen, the Same Predicted Trend for Conductance Versus Polarizability Is Also Observed for Substituted Benzene Rings. The Substituted Benzene Rings 1 to 8 Are, *ph-F*, *p-Cl*, *ph-*CHF_2, *ph-*OCH_3, *ph-SH*, *ph-*NO_2, *ph-*CH_2Cl and *ph-*CCl_3 Respectively.

(Figure 2.1). Importantly, (because of its rigidity) substituents ranging from electron withdrawing group (EWG) to electron donating group (EDG), imposed negligible structural effects on the benzene ring. This helped us maintain similar geometries for the electrodes, anchoring groups and the molecular bridge in all systems; avoiding, to a large extent, the effect of the linkers on the conductance. Figure 3.3 suggests that, qualitatively, the results follow the predicted trend. The conductance values are also consistent with experimental measurements (Martin et al., 2008).

Next, we analyzed the results presented in a recent paper by Breslow and coworkers who have measured the conductance of different molecular wires (Figure 3.4) with a five-membered rings of furan or thiophene (Chen et al., 2014). Their results showed a consistently higher conductance for analogous thiophene systems that was attributed to a decrease of aromaticity (Chen et al., 2014). We have computed the polarizability of these systems and plotted the experimental conductance against the calculated polarizability. We are sticking to the same notation that was used in the experimental papers to facilitate cross checking of the systems. The computational details can be found in the supporting information. The results are displayed in Figure 3.5 and they clearly suggest that, the behaviour of these junctions is controlled by the same type of physics included in our simple dielectric model.

To further investigate the robustness of our correlation between polarizability and conductance, we have chosen a series of molecules that were studied experimentally by Meisner and coworkers (Meisner et al., 2012). The molecular wires are functionalized with para-para or para-meta di-methyl sulfide groups at both of the phenyl termini as can be seen in Figure 3.6. The difference in the conductances is justified by the difference in the "linker" group properties and binding interactions. Figure 3.7 summarizes the results. In this case, the polarizability of linker+molecule is calculated. It can be seen that for each family of molecules the increase in polarizability corresponds to a decrease in the conductance. It is also apparent that the conductance of PP_n is systematically higher than that of PM_n. It is known that the nature of bonding

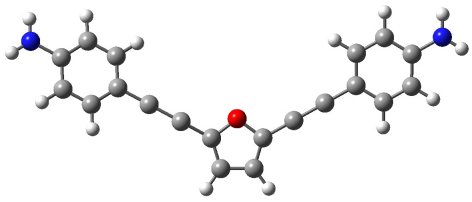

(a) Compound **2**, 2,5-bis(4-aminophenylethinyl)furan.

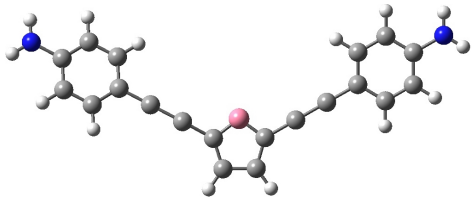

(b) Compound **3**, 2,5-bis(4-aminophenylethinyl)thiophene.

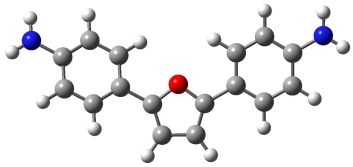

(c) Compound **5**, 2,5-bis-(4-aminophenyl)furan.

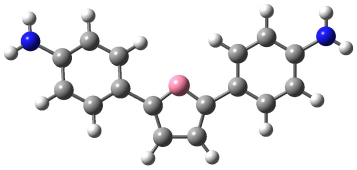

(d) Compound **6**, 2,5-bis(4-aminophenyl)thiophene.

Figure 3.4: The Molecular Wires Studied By Chen et al. These Molecular Wires Contain a Five Membered Ring. The Amino Groups at Both Ends of the Wires Act as the Linker and Connects the Wires to the Gold Electrodes (Chen et al., 2014).

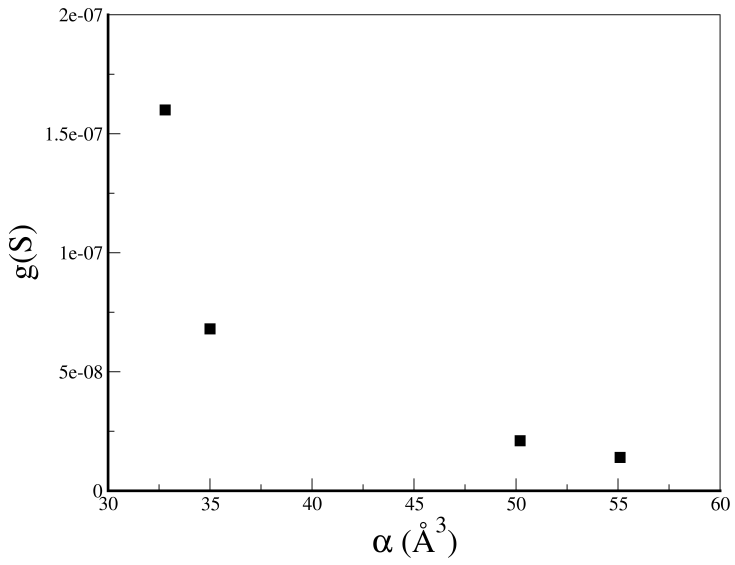

Figure 3.5: Experimentally Measured Conductance vs Calculated Polarizability for Structures **2**,**3** and **5**, **6** of the Systems Studied by Chen et al (Chen et al., 2014).

between the electrode and the linker groups can dramatically affect the conductance (Hong et al., 2012; Chen et al., 2006; Ke et al., 2004). Our polarizability model does not encompass the interaction and electronic coupling between the electrode and the anchoring group. Hence, the difference between the *Au*-*S* bonding and *Au*-*N* and their effect on conductance cannot be captured in our model. In fact, polarizability should clearly be a better descriptor of molecular conductance for weaker electrode-anchoring group interaction, because this weak interaction is a necessary condition for the approximate separability of the conductance in a molecular and an electrode term.

So far, we only discussed electron transport across covalent bonded systems and its relationship with the polarizability. In addition, due to the importance of non-

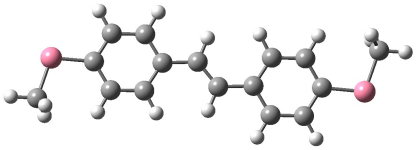

(a) PP1.

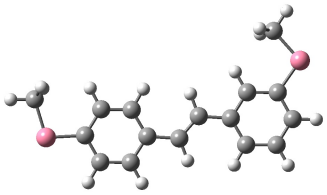

(b) PM1.

Figure 3.6: The Molecular Wires Experimentally Studied by Meisner et al. (Meisner et al., 2012).

covalent interactions between individual molecules in designing nanoelectronic devices based on supramolecular self-assembly, we decided to investigate the electron transport across molecules bound by hydrogen bonds (as one of the most important non-covalent interaction in biology and chemistry) and its relation with polarizability. Therefore the next section, will be about electron transport across the hydrogen bond.

3.3 Hydrogen Bond Electron Transport Property

There is tremendous interest in the design and development of functional nanoelectronic devices based on the principles of controlled organization and supramolecular

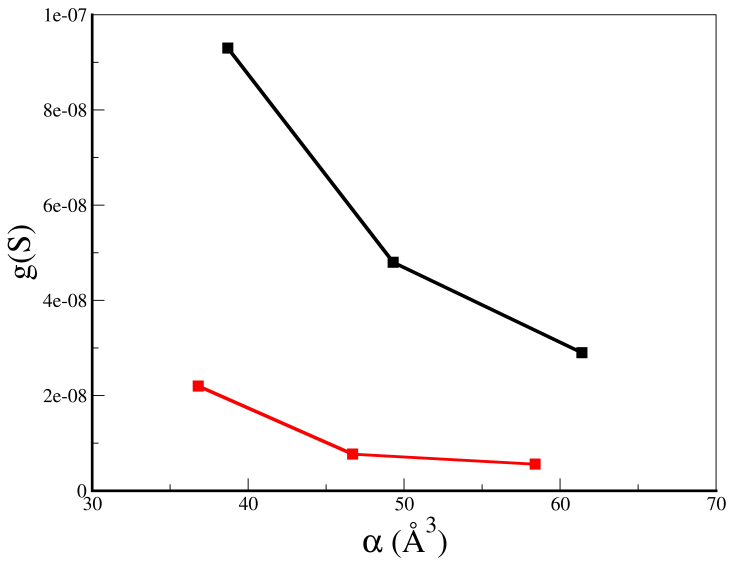

Figure 3.7: Experimentally Measured Conductance of Different Systems from Meisner et al. (Meisner et al., 2012) Versus Calculated Polarizability. It Can Be Seen That PP_n and PM_n (n=1-3) Molecules Approximately Follow the Trend Predicted by the Polarizability Model.

self-assembly (Weiss et al., 2008; Whitesides et al., 2002; Parviz et al., 2003; Boncheva et al., 2002; Yokoyama et al., 2001; Lindsay et al., 2012; Huang et al., 2012; Bath et al., 2013; Kim et al., 2012; Lehn et al., 2013; Pease et al., 2001). This has been largely spurred by the recent demand for electronics in biomedical applications (Lindsay et al., 2012). Thus, non-covalent interacations between individual molecules can lead to functional nanoelectronic devices by controlled organization and self-assembly. Apart from being structurally rigid, these molecular asssemblies should also facilitate electron transfer between the individual molecules. Despite substantial breakthroughs in the context of nucleotide sensing devices (Weiss et al., 2008; Huang et al., 2012;

Chang et al., 2011) there have been relatively few investigations of electron transfer across molecules or molecular assemblies bound by non-covalent interactions (Wu et al., 2008; Holmlin et al., 2001; Slowinski et al., 1997; De Rege et al., 1995). As a result, there is scant information on the nature of electron transport across hydrogen bonds despite it being one of the most widely investigated non-covalent interactions (Jeffrey et al., 1997; Scheiner, 1997; Kim et al., 2000; Lee et al., 2007; Tarakeshwar et al., 2002). In view of the growing relevance of hydrogen bonds in the context of organic electronic devices (Gowacki et al., 2013), there is an urgent need for a systematic study of electronic transport across hydrogen bonding.

A hydrogen bond results from an attractive interaction between the hydrogen atom of a donor-hydrogen covalent bond (D-H) and an electronegative acceptor atom (B) or a polarizable π system (Scheiner, 1997; Kim et al., 2000; Tarakeshwar et al., 2002). Despite their small interaction energies compared to a conventional covalent bond, cooperative and collective effects between hydrogen bonds have known to be extremely useful in direct electronic sensing of chemical and physical processes (Cahen et al., 2005; Paltiel et al., 2010) An important feature of hydrogen bonds is that they are characterized by extremely high polarizabilies (Janoschek et al., 1972), which are further increased in the presence of external electric fields (Eckert et al., 1987). In the context of electron transport across hydrogen bonds, this feature is extremely important because polarizable systems have a soft electron cloud that deforms in response to bias modulation which in turn modulates the tunneling current via changes

in the barrier properties that can be correlated to changes in the local dielectric properties of the media (Natan et al., 2010). Indeed, changes in the conductance of molecules adsorbed on gold electrodes have been extremely useful in measuring their polarizabilities (Moore et al., 2010).

The current investigation was spurred by a recent experimental measurement of electron transfer across hydrogen bonds (Nishino et al., 2013). Even though the magnitude of the conductance was very small ($\sim 10^{-9}$ S), the authors found that at short range, hydrogen bonds conduct electrons better than a covalent σ bond (Nishino et al., 2013). However, the conductance rapidly decays when the electron transfer pathway becomes longer (Nishino et al., 2013). Against this background, we felt it would be interesting to investigate electron transport across hydrogen bonds and examine the role of factors like hydrogen bond length, strength, and polarizabilities in influencing its magnitude. As has been shown in a recent study of the development of nano pH indicator (Granhen et al., 2010), knowledge of some of these factors would provide useful theoretical guidelines for the development of hydrogen bond based functional electronic nanodevices and organic electronics.

As hydrogen bonding systems relevant to organic electronics need to be both structurally rigid and also facilitate electron transport, all the molecules chosen in this study (crotonic acid, propenyl amine, benzoic acid, aniline, pyridine) either possess double bonds or aromatic rings. Since N-H$\cdots$O, O-H$\cdots$O and N-H$\cdots$N are the three most widely prevalent hydrogen bonds in biological systems and organic electronics

(Jeffrey et al., 1997; Gowacki et al., 2013), the carboxyl and amino functional groups were chosen for mediating the hydrogen bonds. In the next sections, I will talk more about these hydrogen bonded complexes, their electron transport properties and their relevance.

3.3.1 The structures of the hydrogen bonded complexes considered in this study

As mentioned above, we were interested in studying hydrogen bonded complexes with N-H···O, O-H···O and N-H···N bonds. Therefore, we chose 5 different monomers including crotonic acid, propenyl amine, benzoic acid, aniline, and pyridine which are enable to form our desirable hydrogen bonds with different strength and electronic properties. Based on the monomers employed in this study, several plausible hydrogen bonded complexes can be obtained. Thus a linear hydrogen bonded complex **1** can result from the interaction of two crotonic acid molecules. In Figure 3.8, the B3LYP/6-311++G(2d,2p) optimized structures of the different hydrogen bonded complexes are displayed. It can be seen that structures **1** and **2** exhibit a O-H···O type of interaction, structures **3** and **4**: a O-H···N type of interaction, structures **5** and **6**: a N-H···O type of interaction and structures **7** and **8**: a N-H···N type of interaction. Thus, the interacting molecules in all the odd-numbered systems involve double bonds and those in the even-numbered systems involve aromatic systems. Though the interaction of two propenyl amine or aniline molecules can result in the formation of a N-H···N hydrogen bond, pyridine was employed as an acceptor because the biologically relevant N-H···N interactions involve a ring nitrogen as an

acceptor atom. Though the hydroxyl functional group of crotonic and benzoic acid can also behave as hydrogen bond acceptors, we did not consider them because the resulting hydrogen bonds are much weaker than those investigated in this stidy. We also investigated a energetically more stable dimeric structure (Figure 3.9) resulting from the interaction of two crotonic or benzoic acid molecules. Though the anti form of carboxyl group is energically less stable than the corresponding syn form, we also carried out an investigation of the interaction of aniline with the anti form of benzoic acid **60**.

3.3.2 Geometries and Energies

The calculated interaction energies (Table 3.1) of the linear hydrogen bonded complexes indicate that the relative magnitude of the strength of the interaction follow the order (N-H$\cdots$O $<$ N-H$\cdots$N $<$ O-H$\cdots$O $<$ O-H$\cdots$N). Interestingly, the calculations involving the smaller 6-31+G* basis set exhibit similar trends as those involving the larger 6-311++G(2d,2p) basis set. Even though, the O-H$\cdots$N hydrogen bonds are the strongest, they are not prevalent in biological systems (Jeffrey, 1997). In the absence of any experimental or theoretical study of the linear hydrogen bonded complexes, it is useful to note that the calculated interaction energies ($\sim$15.5 kcal/mol) of the benzoic acid dimer (**2D**) are in good agreement with earlier experimental and theoretical studies (Lourderaj et al., 2006; Allen et al., 1966). As was noted in an earlier study of the acetic acid dimer (Nakabayashi et al., 2001), the interaction of the linear hydrogen bonded complexes is weaker than the interaction in the corresponding

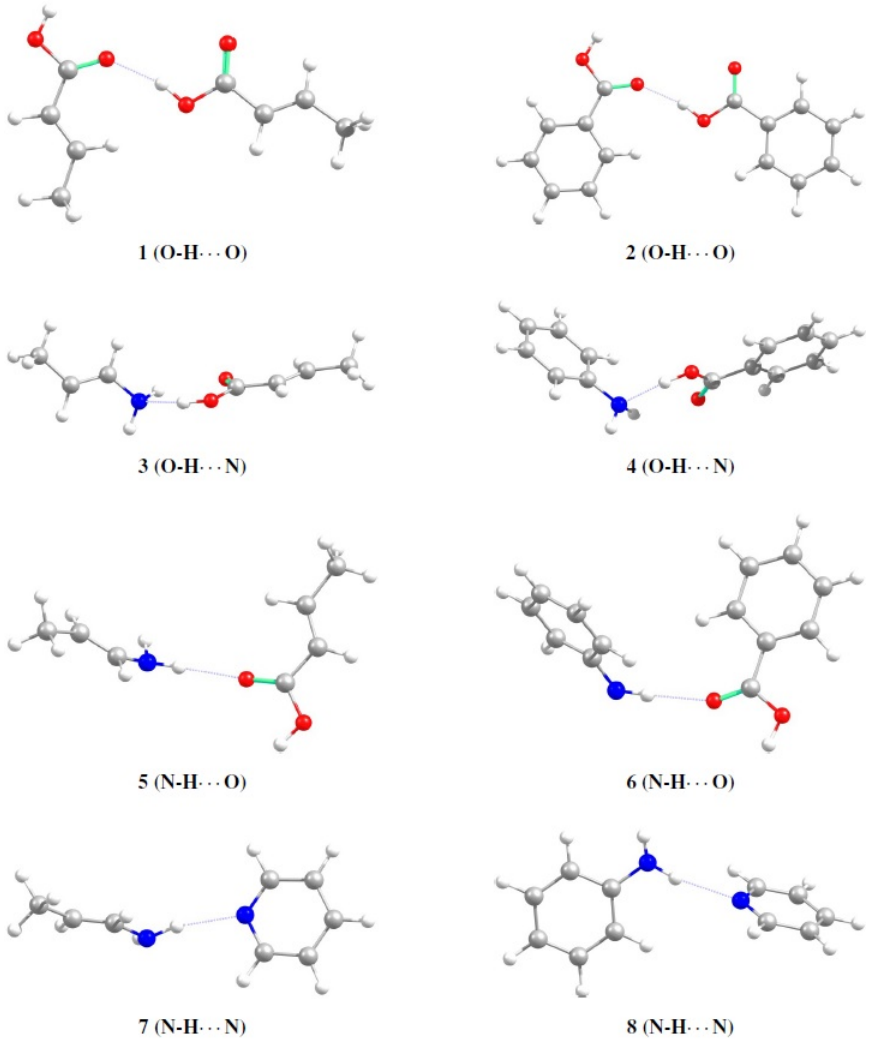

Figure 3.8: B3LYP/6-311++G(2d,2p) Optimized Structures of All Linear Hydrogen Bonded Complexes.

dimeric hydrogen bonded complexes. It is obvious from 3.1 that there is little correlation between the strength and length of the hydrogen bond. Since electron transport across hydrogen bonds is predominantly mediated through quantum-mechanical electron tunneling, it has been earlier mentioned that hydrogen bond length is a relevant

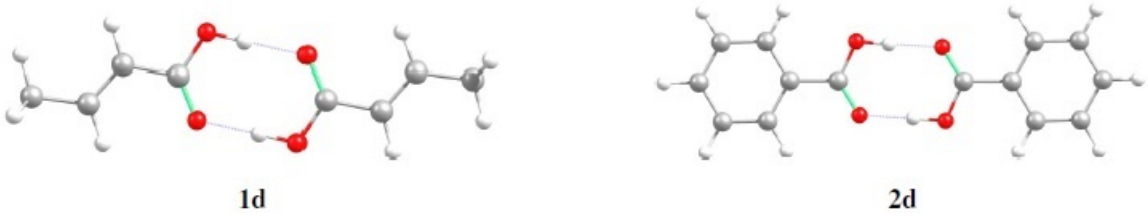

Figure 3.9: B3LYP/6-311++G(2d,2p) Optimized Structures of the Crotonic (**1d**) and Benzoic (**2d**) Acid Dimers.

issue in tunneling (Lindsay, 2012; Huang et al., 2010; Nishino et al., 2013; Lee et al., 2009).

3.3.3 Electronic Transport Characteristics

Before we discuss the electronic transport characteristics of these hydrogen bonded complexes, it is useful to note that the all the monomers have nearly similar highest occupied molecular orbital (HOMO)-lowest unoccupied molecular orbital (LUMO) gaps (Table 3.2). Interesting however is the relative magnitude of the polarizabilities of the donor and acceptor atoms involved in the formation of the hydrogen bond. Since the donor atom is involved in the formation of a covalent bond with the hydrogen atom, its calculated atomic polarizability is substantially smaller than that of the acceptor atom.

With this background, it is useful to examine the electronic characteristics of all the hydrogen bonded complexes investigated in this study (Table 3.3). In recent work, the experimentally observed conductance of hydrogen-bonded ω-carboxyl ethanethiol (HS-$(CH_2)_2$COOH) dimer was found to be 1.5 nS, which was slightly larger than that

Table 3.1: Calculated B3LYP Interaction Energies and Selected Geometry Parameters of Different Hydrogen Bonded System[a]

	6-31+G*					6-311++G(2d,2p)				
System	ΔE	ΔE_B	$\mathbf{r}_{D\cdots A}$	$\mathbf{r}_{D-H}$	$\mathbf{r}_{A\cdots H}$	ΔE	ΔE_B	$\mathbf{r}_{D\cdots A}$	$\mathbf{r}_{D-H}$	$\mathbf{r}_{A\cdots H}$
1(O-H$\cdots$O)	-6.3	-5.5	2.793	0.984	1.840	-5.5	-5.1	2.792	0.981	1.839
2(O-H$\cdots$O)	-6.1	-5.2	2.806	0.982	1.845	-5.3	-4.9	2.804	0.979	1.846
3(O-H$\cdots$N)	-10.1	-8.8	2.809	1.001	1.828	-8.6	-8.2	2.816	0.995	1.840
4(O-H$\cdots$N)	-10.0	-8.6	2.808	1.000	1.824	-8.3	-8.0	2.818	0.994	1.839
5(N-H$\cdots$O)	-3.7	-3.2	3.127	1.015	2.128	-2.8	-2.6	3.175	1.010	2.166
6(N-H$\cdots$O)	-4.0	-3.2	3.130	1.015	2.126	-3.3	-3.0	3.151	1.010	2.142
7(N-H$\cdots$N)	-4.5	-4.0	3.149	1.019	2.151	-3.9	-3.7	3.158	1.015	2.160
8(N-H$\cdots$N)	-4.8	-4.2	3.140	1.019	2.153	-4.2	-4.0	3.147	1.015	2.162
1D(O-H$\cdots$O)$_2$	-16.8	-15.4	2.702	0.999	1.704	-15.8	-15.2	2.654	1.001	1.653
2D(O-H$\cdots$O)$_2$	-17.1	-15.6	2.694	0.999	1.695	-16.0	-15.4	2.648	1.001	1.647
60(N-H$\cdots$O)	-4.2	-3.7	3.126	1.015	2.112	-3.9	-3.7	3.150	1.011	2.140

[a]All energies are in kcal/mol. See Figures 3.8 and 3.9 for description of the various complexes. ΔE and ΔE_B represent the interaction energies without and with BSSE correction, respectively. D, H, and A, are the donor, hydrogen, and acceptor atoms in the hydrogen bond. $r_{D\cdots A}$, $r_{D\text{-}H}$, and $r_{A\cdots H}$ are in the units of Å.

Table 3.2: Calculated B3LYP Orbital Energies, Molecular and Atomic Polarizabilities of Different Hydrogen-Bonded Systems[a]

	6-31+G*			6-311++G(2d,2p)					
System	**H**	**L**	$\Sigma\alpha$	**H**	**L**	$\Sigma\alpha$	α_D	α_H	α_A
Crotonic acid	-7.7	-1.6	41	-7.7	-1.6	44	4.3	4.7	6.3
Propenyl amine	-5.5	0.1	35	-5.6	-0.2	38	3.4	3.7/4.8	3.4
Benzoic acid	-7.4	-1.8	61	-7.5	-1.8	63	3.7	5.1	7.7
Benzoic acid (A)	-7.6	-1.8	61	-7.7	-1.9	63	5.8	2.8	8.1
Aniline	-5.7	-0.3	56	-5.8	-0.4	58	3.8	4.6/4.6	3.8
Pyridine	-7.2	-1.1	45	-7.2	-1.1	46			5.8

[a]H (highest occupied molecular orbital) and L (lowest unoccupied molecular orbital) energies are in eV. $\Sigma\alpha$ is the total molecular polarizability in atomic units (a.u.). α_D, α_H, and α_A are the polarizabilities (a.u.) of the donor, hydrogen, and acceptor atoms in the various monomers.

of a single octanedithiol molecular junction (0.99 nS) (Nishino et al., 2013). The calculated conductance of the benzoic acid dimer (**2D**) optimized at the B3LYP/6-311++G(2d,2p) level of theory is 5.8 nS (Table 3.3). While the higher conductance of **2D** compared to that of ω-carboxyl ethanethiol can be attributed to the fact that the former possesses a conjugated aromatic system, it is useful to note that the calculated conductance of all the hydrogen-bonded complexes reported in this work are of nearly the same order of magnitude. It has been observed that molecular wires exhibit enhanced condutivities possess smaller HOMO-LUMO gaps (Emberly

Table 3.3: Calculated B3LYP Orbital Energies, Molecular and Atomic Polarizabilities of Different Hydrogen-Bonded Systems[a]

	6-31+G*					6-311++G(2d,2p)							
System	**H**	**L**	**H-L**	$\Sigma\alpha$	G	**H**	**L**	**H-L**	α_D	α_H	α_A	$\Sigma\alpha$	G
1	-7.3	-1.9	5.4	83	3.0	-7.3	-1.9	5.4	1.8	1.7	1.9	87	3.9
2	-7.1	-2.1	5.0	124	0.3	-7.1	-2.1	5.0	0.0	0.3	4.8	127	0.8
3	-6.1	-1.3	4.8	77	0.5	-6.1	-1.3	4.8	3.2	2.0	0.2	82	1.4
4	-6.2	-1.5	4.7	118	0.4	-6.3	-1.6	4.7	2.7	2.0	0.5	121	0.1
5	-5.2	-1.8	3.4	76	6.6	-5.1	-1.8	3.3	1.7	1.7	2.0	82	0.3
6	-5.4	-2.0	3.4	117	1.0	-5.4	-2.0	3.4	2.8	2.0	3.2	121	0.4
7	-5.0	-1.4	3.6	81	2.2	-5.1	-1.4	3.7	1.1	1.6	1.2	85	1.9
8	-5.2	-1.4	3.8	101	0.3	-5.3	-1.4	3.9	1.7	1.9	0.5	105	0.2
1D	-7.6	-1.6	6.0	84	41.4	-7.7	-1.6	6.0	3.4	1.8	2.5	88	9.4
2D	-7.4	-1.8	5.5	125	12.6	-7.4	-1.9	5.5	2.7	1.8	2.4	129	5.8
60	-5.1	-2.1	2.9	119	0.4	-5.2	-2.1	3.0	1.7	1.5	2.0	123	0.8

[a]H (highest occupied molecular orbital), L (lowest unoccupied molecular orbital), and H-L (HOMO-LUMO gap) energies are in eV. $\Sigma\alpha$ is the total molecular polarizability in atomic units (a.u.). α_D, α_H, and α_A are the polarizabilities (a.u.) of the donor, hydrogen, and acceptor atoms in the hydrogen bond. The molecular conductance (G) is in units of nanoSiemens (nS).

et al., 1998; Tian et al., 1998; Kemp et al., 1994; Cohen et al., 2007; Perepichka et al., 2005). In Table 3.3, it can be seen that the calculated conductances of these hydrogen bonded complexes do not exhibit any correlation to the corresponding HOMO-LUMO gaps. It is however interesting to note that hydrogen bonded complexes resulting from the interaction of aromatic molecules exhibit lower conductance than those involving the interaction of molecules possessing alkenyl double bonds. Given the relation between conductance and polarizabilities, we plot the calculated molecular polarizabilties and the corresponding conductances in Figure 3.10. It is obvious from the plot that for complexes exhibiting identical hydrogen bonding interactions, an enhanced conductivity is associated with a smaller polarizability. On a similar note, it can be noted that a larger conductance across the hydrogen bond corresponds to a smaller magnitude of polarizability of the acceptor atom. While we highlight this correlation in more detail in a subsequent section, the above correlation can be construed to mean that a larger change in the polarizabilty of the acceptor atom in the dimer compared to its polarizability in the monomer is associated with a higher conductivity.

3.3.4 Extensions to systems of biological relevance

The hydrogen bond between *p*-benzosemiquinone and imidazole is vital in facilitating electron transfer in energy conversion reactions involving most biological systems (Ohashi et al., 2010; Saito, et al., 2013) It is therefore interesting to examine the nature of charge transport across this hydrogen bond. Since previous work

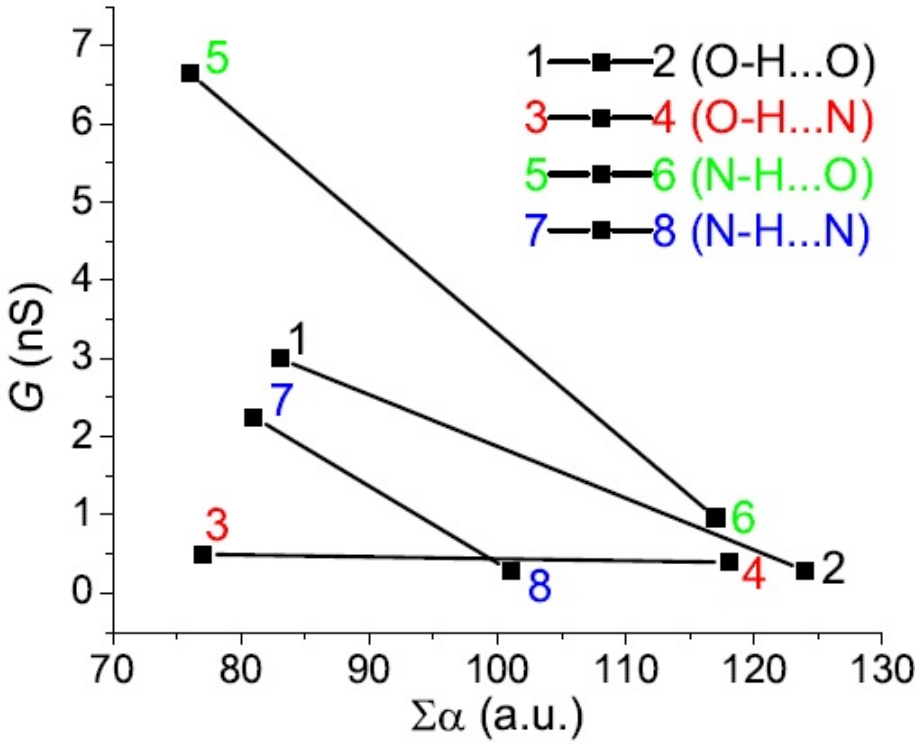

Figure 3.10: Correlation of the Calculated Molecular Polarizabilities (a.u.) and the Molecular Conductances (nS) of All the Hydrogen-Bonded Complexes.

has shown that the presence of substituents greatly influence the electronic transport properties of the molecular devices (Zhang et al., 2009; Fan et al., 2010; Lu et al., 2004), we also examined the role of substituents on the nature of the hydrogen bond and the resulting transport characteristics. The presence of a hydroxyl group in the *para* position relative to the acceptor oxygen of the hydrogen bond implies that electron withdrawing (NO_2) and electron donating (NH_2) groups can be substituted either on the imidazole ring or the *ortho* and *meta* positions of the phenyl ring. In Figure 3.11, the B3LYP/6-31+G* optimized structures of the various substituted *p*-benzosemiquinone-imidazole complexes. It should be noted that all these complexes

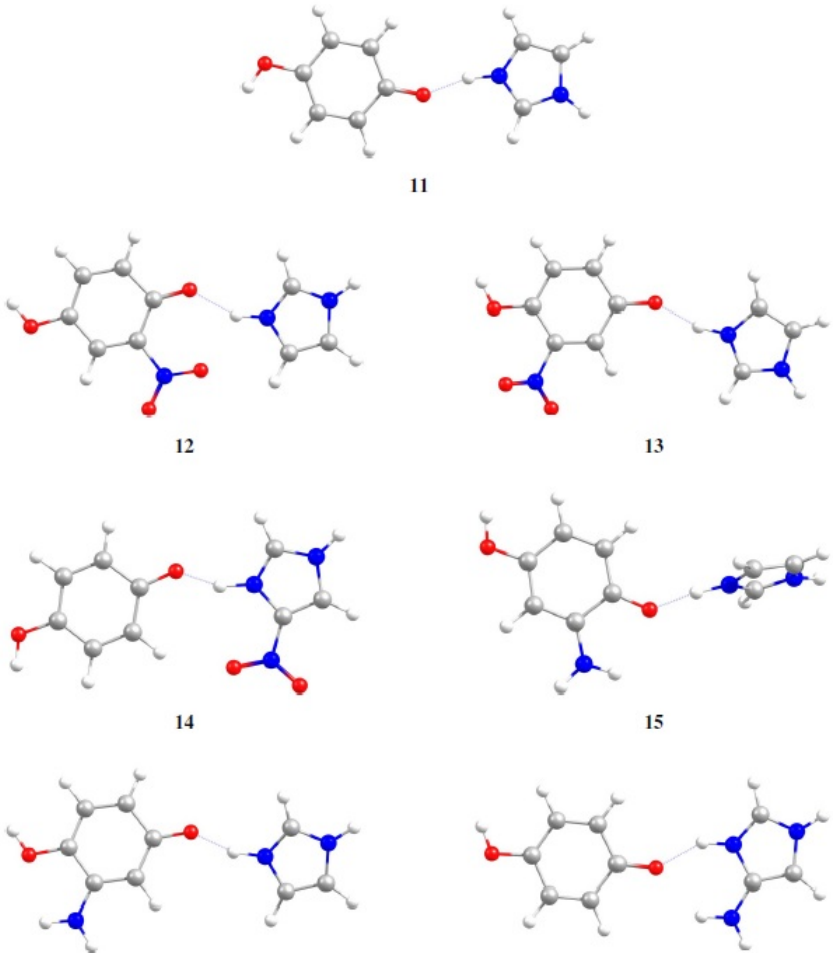

Figure 3.11: B3LYP/6-31+G* Optimized Structures of All the p-Benzosemiquinone-Imidazole Hydrogen- Bonded Complexes.

possess a single positive charge and are open-shell spin doublets. As was seen earlier, the interaction energies HOMO-LUMO gaps are not very informative on the nature of electron transport. Hence we only present the polarizabilties, selected geometrical parameters, and the corresponding conductances in Table 3.4. It can be seen that the presence of an electron-withdrawing or electron-donating substituent on the imidazole ring has little effect on the observed conductances. However, the presence

Table 3.4: Calculated Polarizabilties, Selected Geometrical Parameters, and Molecular Conductance of the p-Benzosemiquinone-Imidazole Hydrogen-Bonded System[a]

System	α_N	α_H	α_O	$\Sigma\alpha$	r_{N-H}	$r_{O\cdots H}$	$r_{O\cdots N}$	G
11	-0.4	1.2	3.3	87	1.052	1.623	2.647	18.7
12	-0.6	0.9	4.0	99	1.039	1.775	2.753	2.4
13	-0.8	1.0	5.1	99	1.045	1.668	2.696	77.8
14	0.0	1.2	2.8	100	1.101	1.484	2.541	7.3
15	-0.5	1.2	3.0	94	1.070	1.561	2.632	44.0
16	-0.6	1.3	4.4	96	1.067	1.560	2.600	6.9
17	-0.1	1.1	2.4	95	1.036	1.759	2.692	8.1

[a]See Figure 3.11 for description of the various complexes. $\Sigma\alpha$ is the total molecular polarizability in atomic units (a.u.). α_D, α_H, and α_A are the polarizabilities (a.u.) of the donor, hydrogen, and acceptor atoms in the hydrogen bond. The molecular conductance (G) is in units of nanoSiemens (nS).

of an electron-withdrawing group at the *meta* position or a electron-donating group at the *ortho* position of the phenyl ring enhances the observed conductances. This effect is easy to understand in the context of activating and deactivating groups in electrophilic aromatic substitution reactions (Olah 1971). Thus, the presence of an electron withdrawing (NO_2) group at the *ortho* position leads to a partial positive charge on the carbon attached to acceptor oxygen atom. The resulting decrease in the electron density of the acceptor oxygen atom leads to a weakening of the O$\cdots$H-N hydrogen bond. Thus, the $r_{O\cdots N}$ in (**12**) is 2.753 $\mathring{A}$ compared to 2.647 $\mathring{A}$ in the

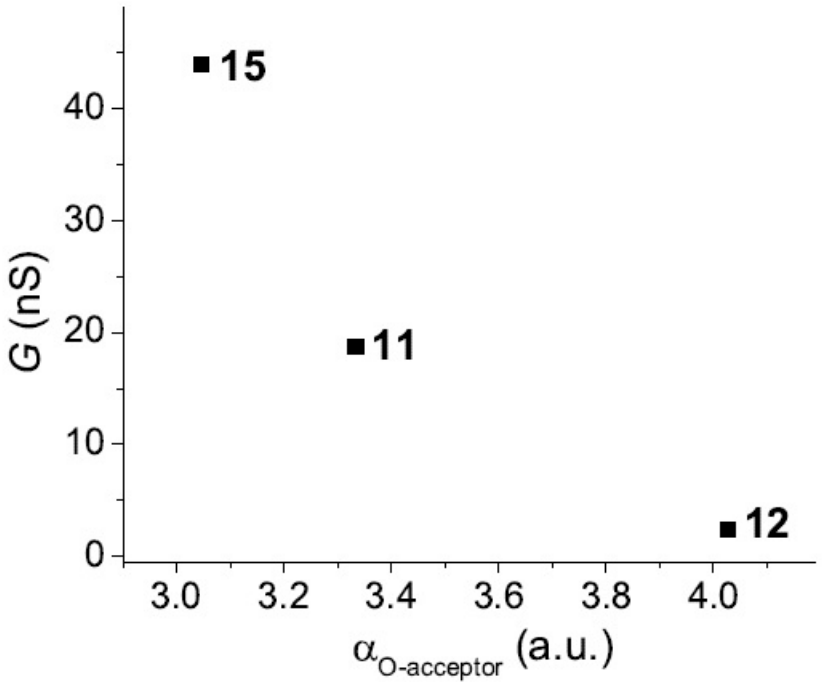

Figure 3.12: Correlation of the Calculated Atomic Polarizabilities (a.u.) of the Acceptor Oxygen Atom and the Molecular Conductances (nS) of Ortho-Substituted p-Benzosemiquinone-Imidazole Hydrogen-Bonded Complexes.

unsubstituted *p*-benzosemiquinone-imidazole (**11**) complex. On a similar note, the enhancement of the condutance in **15** can be explained. Since the electron density on the acceptor oxygen atom is influenced by the presence of the substituents, it can be expected that its polarizability would reflect the observed conductance. It can indeed be seen in Figure 3.12, that the polarizabilities of the acceptor oxygen atom exhibit an inverse correlation to the observed conductance.

Chapter 4

CONCLUSION AND FUTURE WORKS

In this work we have explored the rather substantial computational evidence of an existing correlation between the static isotropic molecular polarizability and the molecular contribution to the zero-voltage conductance of a molecular junction. We have also examined the physical origin of such a correlation via a model that connects the local dielectric properties of the junction to its transport behaviour via changes in the effective height of the associated tunneling barrier. The model was computationally tested with various covalent and non-covalent bonded systems. It's worth mentioning that our model only provides some physically plausible arguments and does not constitute a first-principle theory, however to our knowledge it is the first systematic attempt in trying to explicitly describe molecular conductance in terms of polarizability.

Our results, together with the fact that there is a direct relationship between molecular conductance and electron transfer rate (Nitzan, 2001), which is valid for low bias, point in the direction that it should be possible to reformulate Marcus theory of electron transfer directly in terms of the frequency-dependent dielectric response, a goal we are currently working on. Using molecular polarizability as a descriptor of conductance may also have important implications for the theory of molecular dielectrics.

REFERENCES

Aviram, A., and M. A. Ratner. "Molecular rectifiers." Chemical Physics Letters 29.2 (1974): 277-283.

Cui, X. D., A. Primak, X. Zarate, J. Tomfohr, O. F. Sankey, A. L. Moore, T. A. Moore, D. Gust, G. Harris, and S. M. Lindsay. "Reproducible measurement of single-molecule conductivity." Science 294.5542 (2001): 571-574.

Smit, R. H. M., Y. Noat, C. Untiedt, N. D. Lang, M. C. Van Hemert, and J. M. Van Ruitenbeek."Measurement of the conductance of a hydrogen molecule." Nature 419.6910 (2002): 906-909.

Xu, B., and N. J. Tao. "Measurement of single-molecule resistance by repeated formation of molecular junctions." Science 301.5637 (2003): 1221-1223.

Reed, Mark A., C. Zhou, C. J. Muller, T. P. Burgin, and J. M. Tour. "Conductance of a molecular junction." Science 278.5336 (1997): 252-254.

Porath, D., A. Bezryadin, S. de Vries, and C. Dekker. "Direct measurement of electrical transport through DNA molecules." Nature 403.6770 (2000): 635-638.

Evers, F., F. Weigend, and M. Koentopp. "Conductance of molecular wires and transport calculations based on density-functional theory." Physical Review B 69.23 (2004): 235411.

Stokbro, K., J. Taylor, M. Brandbyge, J. L. Mozos, and P. Ordejon. "Theoretical study of the nonlinear conductance of Di-thiol benzene coupled to Au (111) surfaces via thiol and thiolate bonds." Computational Materials Science 27.1 (2003): 151-160.

Simmons, J. G. "Generalized formula for the electric tunnel effect between similar electrodes separated by a thin insulating film." Journal of Applied Physics 34.6 (1963): 1793-1803.

Lang, N. D. "Apparent barrier height in scanning tunneling microscopy." Physical Review B 37.17 (1988): 10395.

Tersoff, J., and D. R. Hamann. "Theory of the scanning tunneling microscope." Physical Review B 31.2 (1985): 805.

Bardeen, J. "Tunnelling from a many-particle point of view." Physical Review Letters 6.2 (1961): 57.

Landauer, R. "Electrical resistance of disordered one-dimensional lattices." Philosophical Magazine 21.172 (1970): 863-867.

Imry Y. 1997. Introduction to Mesoscopic Physics. Oxford, UK: Oxford Univ. Press

Miller, W. H. "Semiclassical Limit of Quantum Mechanical Transition State Theory for Non-Separable Systems." The Journal of chemical physics 62, 1899-1906 (1975)

Miller, W. H., D. S. Steven, and J. W. Tromp. "Quantum mechanical rate constants for bimolecular reactions." The Journal of chemical physics 79.10 (1983): 4889-4898.

Galperin, M., M. A. Ratner, and A. Nitzan. "Hysteresis, switching, and negative differential resistance in molecular junctions: a polaron model." Nano letters 5.1 (2005): 125-130.

Mujica, V., M. Kemp, and M. A. Ratner. "Electron conduction in molecular wires. I. A scattering formalism." The Journal of chemical physics 101.8 (1994): 6849-6855.

Newns, D. M. "Self-consistent model of hydrogen chemisorption." Physical Review 178.3 (1969): 1123.

de Andrade, P. CP., and J. N. Onuchic. "Generalized pathway model to compute and analyze tunneling matrix elements in proteins." The Journal of chemical physics 108.10 (1998): 4292-4298.

Magoga, M., and C. Joachim. "Conductance and transparence of long molecular wires." Physical Review B 56.8 (1997): 4722.

Yaliraki, S. N., M. Kemp, and M. A. Ratner. "Conductance of molecular wires: influence of molecule-electrode binding." Journal of the American Chemical Society 121.14 (1999): 3428-3434.

Moresco, F., L. Gross, M. Alemani, K. H. Rieder, H. Tang, A. Gourdon, and C. Joachim "Probing the different stages in contacting a single molecular wire." Physical review letters 91.3 (2003): 036601.

Chen, F., J. Hihath, Z. Huang, X. Li, and N. J. Tao. "Measurement of single-molecule conductance." Annual Review of Physical Chemistry 58 (2007): 535-564.

Kalakodimi, R. "Carbon/molecule/metal molecular electronic junctions: the importance of contacts." Faraday Discussions 131 (2006): 33-43.

Xue, Y., and M. A. Ratner. "Microscopic study of electrical transport through individual molecules with metallic contacts. I. Band lineup, voltage drop, and high-field transport." Physical Review B 68.11 (2003): 115406.

Ke, S. H., H. U. Baranger, and W. Yang. "Molecular conductance: Chemical trends of anchoring groups." Journal of the American Chemical Society 126.48 (2004): 15897-15904.

Mller, K. H. "Effect of the atomic configuration of gold electrodes on the electri-

cal conduction of alkanedithiol molecules." Physical Review B 73.4 (2006): 045403.

Beebe, J. M., V. B. Engelkes, L. L. Miller, and C. D. Frisbie. "Contact resistance in metal-molecule-metal junctions based on aliphatic SAMs: Effects of surface linker and metal work function." Journal of the American Chemical Society 124.38 (2002): 11268-11269.

Hu, Y., Y. Zhu, H. Gao, and H. Guo. "Conductance of an ensemble of molecular wires: A statistical analysis." Physical review letters 95.15 (2005): 156803.

Basch, H., R. Cohen, and M. A. Ratner. "Interface geometry and molecular junction conductance: Geometric fluctuation and stochastic switching." Nano letters 5.9 (2005): 1668-1675.

Schmickler, W., and C. Widrig. "The investigation of redox reactions with a scanning tunneling microscope: experimental and theoretical aspects." Journal of Electroanalytical Chemistry 336.1 (1992): 213-221.

Kuznetsov, A. M., P. Sommer-Larsen, and J. Ulstrup. "Resonance and environmental fluctuation effects in STM currents through large adsorbed molecules." Surface science 275.1 (1992): 52-64.

Weiss, E. A., M. J. Tauber, R. F. Kelley, M. J. Ahrens, M. A. Ratner, and M. R. Wasielewski. "Conformationally gated switching between superexchange and hopping within oligo-p-phenylene-based molecular wires." Journal of the American Chemical Society 127.33 (2005): 11842-11850.

Nitzan, A. "Electron transmission through molecules and molecular interfaces." Annual Review of Physical Chemistry 52.1 (2001): 681-750.

Selzer, Y., M. A. Cabassi, T. S. Mayer, and D. L. Allara. "Thermally activated conduction in molecular junctions." Journal of the American Chemical Society 126.13 (2004): 4052-4053.

Haiss, W., H. V. Zalinge, D. Bethell, J. Ulstrup, D. J. Schiffrin, and R. J. Nichols. "Thermal gating of the single molecule conductance of alkanedithiols." Faraday discussions 131 (2006): 253-264. "Thermal gating of the single molecule conductance of alkanedithiols." Faraday discussions 131 (2006): 253-264.

Di Ventra, M., S. G. Kim, S. T. Pantelides, and N. D. Lang. "Temperature effects on the transport properties of molecules." Physical review letters 86.2 (2001): 288.

Mantooth, B. A., and P. S. Weiss. "Fabrication, assembly, and characterization of molecular electronic components." Proceedings of the IEEE 91.11 (2003): 1785-1802.

Metzger, R. M. "Unimolecular electrical rectifiers." Chemical reviews 103.9 (2003):

3803-3834.

Liebsch A. 1997. Electronic Excitations at Metal Surfaces, pp. 548. New York: Plenum.

Lang, N. D. "Resistance of atomic wires." Physical Review B 52.7 (1995): 5335.

Lang, N. D., and P. Avouris. "Carbon-atom wires: charge-transfer doping, voltage drop, and the effect of distortions." Physical review letters 84.2 (2000): 358.

Parr RG., Yang W. 1989. Density Functional Theory of Atoms and Molecules Density Functional Theory of Atoms and Molecules. Oxford, UK: Oxford Univ. Press

Di Ventra, M., S. T. Pantelides, and N. D. Lang. "First-principles calculation of transport properties of a molecular device." Physical Review Letters 84.5 (2000): 979.

Lafferentz, L., F. Ample, H. Yu, S. Hecht, C. Joachim, and L. Grill "Conductance of a single conjugated polymer as a continuous function of its length." Science 323.5918 (2009): 1193-1197.

Galperin, M., M. A. Ratner, A. Nitzan, and A. Troisi. "Nuclear coupling and polarization in molecular transport junctions: beyond tunneling to function." Science 319.5866 (2008): 1056-1060.

Nitzan, A., and M. A. Ratner. "Electron transport in molecular wire junctions." Science 300.5624 (2003): 1384-1389.

Joachim, C., J. K. Gimzewski, and A. Aviram. "Electronics using hybrid-molecular and mono-molecular devices." Nature 408.6812 (2000): 541-548.

Tao, N. J. "Electron transport in molecular junctions." Nature Nanotechnology 1.3 (2006): 173-181.

Liu, Z.-F., S. Wei, H. Yoon, O. Adak, I. Ponce, Y. Jiang, W.-D. Jang, L. M. Campos, L. Venkataraman, and J. B. Neaton. "Control of Single-Molecule Junction Conductance of Porphyrins via a Transition-Metal Center." Nano Letters (2014).

Hrtle, R., C. Benesch, and M. Thoss. "Vibrational nonequilibrium effects in the conductance of single molecules with multiple electronic states." Physical review letters 102.14 (2009): 146801.

Bergfield, J. P., and C. A. Stafford. "Many-body theory of electronic transport in single-molecule heterojunctions." Physical Review B 79.24 (2009): 245125.

Baer, R., and D. Neuhauser. "Many-body scattering formalism of quantum molecular conductance." Chemical physics letters 374.5 (2003): 459-463.

Nitzan A. 2006. Chemical Dynamics in Condensed Phases : Relaxation, Transfer and Reactions in Condensed Molecular Systems: Relaxation, Transfer and Reactions in Condensed Molecular Systems. Oxford, UK: Oxford Univ. Press

Magoga, M., and C. Joachim. "Conductance and transparence of long molecular wires." Physical Review B 56.8 (1997): 4722.

Xue, Y., S. Datta, and M. A. Ratner. "Charge transfer and band lineup in molecular electronic devices: A chemical and numerical interpretation." The Journal of Chemical Physics 115.9 (2001): 4292-4299.

Tomfohr, J. K., and O. F. Sankey. "Complex band structure, decay lengths, and Fermi level alignment in simple molecular electronic systems." Physical Review B 65.24 (2002): 245105.

Pauly, F., J. K. Viljas, J. C. Cuevas, and G. Schn. "Density-functional study of tilt-angle and temperature-dependent conductance in biphenyl dithiol single-molecule junctions." Physical Review B 77.15 (2008): 155312.

McDermott, S., C. B. George, G. Fagas, J. C. Greer, and M. A. Ratner "Tunnel currents across silane diamines/dithiols and alkane diamines/dithiols: A comparative computational study." The Journal of Physical Chemistry C 113.2 (2008): 744-750.

Kamenetska, M., S. Y. Quek, A. C. Whalley, M. L. Steigerwald, H. J. Choi, S. G. Louie, C. Nuckolls, M. S. Hybertsen, J. B. Neaton, and L. Venkataraman. "Conductance and geometry of pyridine-linked single-molecule junctions." Journal of the American Chemical Society 132.19 (2010): 6817-6821.

Brkle, M., J. K. Viljas, D. Vonlanthen, A. Mishchenko, G. Schn, M. Mayor, T. Wandlowski, and F. Pauly. "Conduction mechanisms in biphenyl dithiol single-molecule junctions." Physical Review B 85.7 (2012): 075417.

Venkataraman, L., J. E. Klare, C. Nuckolls, M. S. Hybertsen, and M. L. Steigerwald. "Dependence of single-molecule junction conductance on molecular conformation." Nature 442.7105 (2006): 904-907.

Gonzalez, C., V. Mujica, and M. A. Ratner. "Modeling the electrostatic potential spatial profile of molecular junctions." Annals of the New York Academy of Sciences 960.1 (2002): 163-176.

Mujica, V., A. E. Roitberg, and M. A. Ratner. "Molecular wire conductance: Electrostatic potential spatial profile." The Journal of Chemical Physics 112.15 (2000): 6834-6839.

Kiguchi, M., H. Nakamura, Y. Takahashi, T. Takahashi, and T. Ohto. "Effect of anchoring group position on formation and conductance of a single disubstituted benzene molecule bridging Au electrodes: change of conductive molecular orbital and

electron pathway." The Journal of Physical Chemistry C 114.50 (2010): 22254-22261.

Park, Y. S., A. C. Whalley, M. Kamenetska, M. L. Steigerwald, M. S. Hybertsen, C. Nuckolls, and L. Venkataraman. "Contact chemistry and single-molecule conductance: A comparison of phosphines, methyl sulfides, and amines." Journal of the American Chemical Society 129.51 (2007): 15768-15769.

Chen, F., X. Li, J. Hihath, Z. Huang, and N. Tao. "Effect of anchoring groups on single-molecule conductance: comparative study of thiol-, amine-, and carboxylic-acid-terminated molecules." Journal of the American Chemical Society 128.49 (2006): 15874-15881.

Gonzalez, C., V. Mujica, and M. A. Ratner. "Modelling the electrostatic potential spatial profile of molecular junctions." Annals of the New York Academy of Sciences 960.1 (2002): 163-176.

Metzger, R. M. "Unimolecular electrical rectifiers." Chemical reviews 103.9 (2003): 3803-3834.

Natan, A., N. Kuritz, and L. Kronik. "Polarizability, Susceptibility, and Dielectric Constant of NanometerScale Molecular Films: A Microscopic View." Advanced Functional Materials 20.13 (2010): 2077-2084.

Bergren, A. J., R. L. McCreery, S. R. Stoyanov, S. Gusarov, and A. Kovalenko. "Electronic characteristics and charge transport mechanisms for large area aromatic molecular junctions." The Journal of Physical Chemistry C 114.37 (2010): 15806-15815.

Mujica, V., and M. A. Ratner. "Currentvoltage characteristics of tunneling molecular junctions for off-resonance injection." Chemical Physics 264.3 (2001): 365-370.

Munn, R. W., and P. L. A. Popelier. "Distributed polarizability analysis for para-nitroaniline and meta-nitroaniline: Functional group and charge-transfer contributions." The Journal of chemical physics 120.24 (2004): 11479-11486.

Munn, R. W., P. LA Popelier, J. N. Coleman, B. Foley, and W. J. Blau. "Distributed response analysis of conductive behavior in single molecules." Proceedings of the National Academy of Sciences of the United States of America 99.Suppl 2 (2002): 6514-6517.

Neese, F. "The ORCA program system." Wiley Interdisciplinary Reviews: Computational Molecular Science 2.1 (2012): 73-78.

Becke, A. D. "Densityfunctional thermochemistry. III. The role of exact exchange." The Journal of Chemical Physics 98.7 (1993): 5648-5652.

Lee, C., W. Yang, and R. G. Parr. "Development of the Colle-Salvetti correlation-

energy formula into a functional of the electron density." Physical Review B 37.2 (1988): 785.

Krishnan, R. B. J. S., J. S. Binkley, R. Seeger, and J. A. Pople. "Self-consistent molecular orbital methods. XX. A basis set for correlated wave functions." The Journal of Chemical Physics 72.1 (1980): 650-654.

Clark, T., J. Chandrasekhar, G. W. Spitznagel, and P. V. R. Schleyer. "Efficient diffuse function-augmented basis sets for anion calculations. III. The $3-21+G$ basis set for first-row elements, LiF." Journal of Computational Chemistry 4.3 (1983): 294-301.

Frisch, M. J., J. A. Pople, and J. S. Binkley. "Self-consistent molecular orbital methods 25. Supplementary functions for Gaussian basis sets." The Journal of chemical physics 80.7 (1984): 3265-3269.

Curtiss, L. A., K. Raghavachari, P. C. Redfern, V. Rassolov, and J. A. Pople. "Gaussian-3 (G3) theory for molecules containing first and second-row atoms." The Journal of chemical physics 109.18 (1998): 7764-7776.

Hazra, M. K., J. S. Francisco, and A. Sinha. "Computational study of hydrogen-bonded complexes of $HOCO$ with acids: $HOCO...HCOOH$, $HOCO...H_2SO_4$, and $HOCO...H_2CO_3$." The Journal of chemical physics 137.6 (2012): 064319.

Rustad, J. R., W. H. Casey, Q.-Z. Yin, E. J. Bylaska, A. R. Felmy, S. A. Bogatko, V. E. Jackson, and D. A. Dixon. "Isotopic fractionation of Mg^{2+} (aq), Ca^{2+} (aq), and Fe^{2+} (aq) with carbonate minerals." Geochimica et cosmochimica acta 74.22 (2010): 6301-6323.

Foreman, J. P., and A. P. Monkman. "Theoretical investigations into the structural and electronic influences on the hydrogen bonding in doped polyaniline." The Journal of Physical Chemistry A 107.38 (2003): 7604-7610.

Li G. P., B. Reinhart and I. P. Hamilton "The complex of HF_2^- and H_2O: A theoretical study." The Journal of chemical physics 115 (2001): 5883.

Boys, S. F., and F. de Bernardi. "The calculation of small molecular interactions by the differences of separate total energies. Some procedures with reduced errors." Molecular Physics 19.4 (1970): 553-566.

Marenich, A. V., C. J. Cramer, and D. G. Truhlar. "Reduced and quenched polarizabilities of interior atoms in molecules." Chemical Science 4.6 (2013): 2349-2356.

Soler, J. M., E. Artacho, J. D. Gale, A. Garca, J. Junquera, P. Ordejn, and D. Snchez-Portal. "The SIESTA method for ab initio order-N materials simulation." Journal of Physics: Condensed Matter 14.11 (2002): 2745.

Datta, S. "Nanoscale device modeling: the Greens function method." Superlattices and Microstructures 28.4 (2000): 253-278.

Ferry DK., SM. Goodnick, and J. Bird. (2009) Transport in Nanostructures (2nd Ed.). New York: Cambridge University Press.

Landauer R. IBM J. Res. Dev. 1957;1:23.

Bttiker, M. "Four-terminal phase-coherent conductance." Physical Review Letters 57.14 (1986): 1761.

Perdew, John P., and A. Zunger. "Self-interaction correction to density-functional approximations for many-electron systems." Physical Review B 23.10 (1981): 5048.

Zimbovskaya, N. A., and M. R. Pederson. "Electron transport through molecular junctions." Physics Reports 509.1 (2011): 1-87.

Maniu, D., V. Chis, M. Baia, F. Toderas, and S. Astilean. "Density functional theory investigation of p-aminothiophenol molecules adsorbed on gold nanoparticles." Journal of Optoelectronics and Advanced Materials 9.3 (2007): 733.

Kaliginedi, V., P. Moreno-Garca, H. Valkenier, W. Hong, V. M. Garca-Suarez, P. Buiter, J. LH. Otten, J. C. Hummelen, C. J. Lambert, and T. Wandlowski. "Correlations between molecular structure and single-junction conductance: A case study with oligo (phenylene-ethynylene)-type wires." Journal of the American Chemical Society 134.11 (2012): 5262-5275.

Haiss, W., C. Wang, I. Grace, A. S. Batsanov, D. J. Schiffrin, S. J. Higgins, M. R. Bryce, C. J. Lambert, and R. J. Nichols. "Precision control of single-molecule electrical junctions." Nature materials 5.12 (2006): 995-1002.

Martin, S., I. Grace, M. R. Bryce, C. Wang, R. Jitchati, A. S. Batsanov, S. J. Higgins, C. J. Lambert, and R. J. Nichols. "Identifying diversity in nanoscale electrical break junctions." Journal of the American Chemical Society 132.26 (2010): 9157-9164.

Artacho, E., E. Anglada, O. Diguez, J. D. Gale, A. Garca, J. Junquera, R. M. Martin, P. Ordejon, J. M. Pruneda, D. S. anchez-Portal, and J. M. Soler. "The SIESTA method; developments and applicability." Journal of Physics: Condensed Matter 20.6 (2008): 064208.

Hohenberg, P., and W. Kohn. "Inhomogeneous electron gas." Physical review 136.3B (1964): B864.

Kohn, W., and L. J. Sham. "Self-consistent equations including exchange and correlation effects." Physical Review 140.4A (1965): A1133.

Perdew, J. P., and Y. Wang. "Accurate and simple analytic representation of the

electron-gas correlation energy." Physical Review B 45.23 (1992): 13244.

Harrison, N. M., "An Introduction to Density Functional Theory." In Computational Materials Science, Catlow; Kotomin, Eds. IOS Press 187 (2003).

Ditchfield, R. H. W. J., W. J. Hehre, and J. A. Pople. "Self-consistent molecularorbital methods. IX. An extended Gaussiantype basis for molecular-orbital studies of organic molecules." The Journal of Chemical Physics 54.2 (1971): 724-728.

Hehre, W. J., R. Ditchfield, and J. A. Pople. "Selfconsistent molecular orbital methods. XII. Further extensions of gaussiantype basis sets for use in molecular orbital studies of organic molecules." The Journal of Chemical Physics 56.5 (1972): 2257-2261.

Hariharan, P. C., and J. A. Pople. "The influence of polarization functions on molecular orbital hydrogenation energies." Theoretica chimica acta 28.3 (1973): 213-222.

Hariharan, P. C., and J. A. Pople. "Accuracy of AH n equilibrium geometries by single determinant molecular orbital theory." Molecular Physics 27.1 (1974): 209-214.

Troullier, N., and J. L. Martins. "Efficient pseudopotentials for plane-wave calculations." Physical Review B 43.3 (1991): 1993.

Xue, Y., S. Datta, and M. A. Ratner. "First-principles based matrix Green's function approach to molecular electronic devices: general formalism." Chemical Physics 281.2 (2002): 151-170.

Junquera, J., . Paz, D. Snchez-Portal, and E. Artacho "Numerical atomic orbitals for linear-scaling calculations." Physical Review B 64.23 (2001): 235111.

Meir, Y., and N. S. Wingreen. "Landauer formula for the current through an interacting electron region." Physical review letters 68.16 (1992): 2512.

Jauho, A.-P., N. S. Wingreen, and Y. Meir. "Time-dependent transport in interacting and noninteracting resonant-tunneling systems." Physical Review B 50.8 (1994): 5528.

Di Ventra, M. Electrical transport in nanoscale systems. Vol. 14. Cambridge: Cambridge University Press, 2008.

Löfås, H. 2013. Computational Studies of Electron Transport in Nanoscale Devices. Acta Universitatis Upsaliensis. Digital Comprehensive Summaries of Uppsala Dissertations from the Faculty of Science and Technology 1090. i-x, 89 pp. Uppsala. ISBN 978-91-554-8781-2.

Galperin, M., M. A. Ratner, and A. Nitzan. "Molecular transport junctions: vibrational effects." Journal of Physics: Condensed Matter 19.10 (2007): 103201.

Pleutin, S., H. Grabert, G.-L. Ingold, and A. Nitzan. "The electrostatic potential profile along a biased molecular wire: A model quantum-mechanical calculation." The Journal of chemical physics 118.8 (2003): 3756-3763.

Natan, A., N. Kuritz, and L. Kronik. "Polarizability, Susceptibility, and Dielectric Constant of Nanometer-Scale Molecular Films: A Microscopic View." Advanced Functional Materials 20.13 (2010): 2077-2084.

Mujica, V., and M. A. Ratner. "Currentvoltage characteristics of tunneling molecular junctions for off-resonance injection." Chemical Physics 264.3 (2001): 365-370.

Martin, R. L., E. R. Davidson, and D. F. Eggers Jr. "Ab initio theory of the polarizability and polarizability derivatives in H_2S." Chemical Physics 38.3 (1979): 341-348.

Li, X., J. He, J. Hihath, B. Xu, S. M. Lindsay, and N. Tao. "Conductance of single alkanedithiols: Conduction mechanism and effect of molecule-electrode contacts." Journal of the American Chemical Society 128.6 (2006): 2135-2141.

Engelkes, V. B., J. M. Beebe, and C. D. Frisbie. "Length-dependent transport in molecular junctions based on SAMs of alkanethiols and alkanedithiols: effect of metal work function and applied bias on tunneling efficiency and contact resistance." Journal of the American Chemical Society 126.43 (2004): 14287-14296.

Liu, H., N. Wang, J. Zhao, Y. Guo, X. Yin, F. YC. Boey, and H. Zhang. "LengthDependent Conductance of Molecular Wires and Contact Resistance in MetalMoleculeMetal Junctions." ChemPhysChem 9.10 (2008): 1416-1424.

Ratkova, E. L., and M. V. Fedorov. "On a relationship between molecular polarizability and partial molar volume in water." The Journal of chemical physics 135.24 (2011): 244109.

Martin, C. A., D. Ding, H. SJ. van der Zant, and J. M. van Ruitenbeek. "Lithographic mechanical break junctions for single-molecule measurements in vacuum: possibilities and limitations." New Journal of Physics 10.6 (2008): 065008.

Chen, W., H. Li, J. R. Widawsky, C. Appayee, L. Venkataraman, and R. Breslow. "Aromaticity decreases single-molecule junction conductance." Journal of the American Chemical Society 136.3 (2014): 918-920.

Meisner, J. S., S. Ahn, S. V. Aradhya, M. Krikorian, R. Parameswaran, M. Steigerwald, L. Venkataraman, and C. Nuckolls. "Importance of Direct Metal-π Coupling in Electronic Transport Through Conjugated Single-Molecule Junctions." Journal of the American Chemical Society 134.50 (2012): 20440-20445.

Hong, W., D. Z. Manrique, P. Moreno-Garcia, M. Gulcur, A. Mishchenko, C. J. Lambert, M. R. Bryce, and T. Wandlowski. "Single molecular conductance of tolanes:

experimental and theoretical study on the junction evolution dependent on the anchoring group." Journal of the American Chemical Society 134.4 (2012): 2292-2304.

Chen, F., X. Li, J. Hihath, Z. Huang, and N. J. Tao. "Effect of anchoring groups on single-molecule conductance: comparative study of thiol-, amine-, and carboxylic-acid-terminated molecules." Journal of the American Chemical Society 128.49 (2006): 15874-15881.

Ke, S.-H., H. U. Baranger, and W. Yang. "Molecular conductance: Chemical trends of anchoring groups." Journal of the American Chemical Society 126.48 (2004): 15897-15904.

Nitzan, A. "A relationship between electron-transfer rates and molecular conduction." The Journal of Physical Chemistry A 105.12 (2001): 2677-2679.

Weiss, P. S. "Functional molecules and assemblies in controlled environments: formation and measurements." Accounts of chemical research 41.12 (2008): 1772-1781.

Whitesides, George M., and Bartosz Grzybowski. "Self-assembly at all scales." Science 295.5564 (2002): 2418-2421.

Amir P., B., D. Ryan, and G. M. Whitesides. "Using self-assembly for the fabrication of nano-scale electronic and photonic devices." Advanced Packaging, IEEE Transactions on 26.3 (2003): 233-241.

Boncheva, M., D. H. Gracias, H. O. Jacobs, and G. M. Whitesides. "Biomimetic self-assembly of a functional asymmetrical electronic device." Proceedings of the National Academy of Sciences 99.8 (2002): 4937-4940.

Yokoyama, T., S. Yokoyama, T. Kamikado, Y. Okuno, and S. Mashiko. "Selective assembly on a surface of supramolecular aggregates with controlled size and shape." Nature 413.6856 (2001): 619-621.

Lindsay, S. "Biochemistry and semiconductor electronicsthe next big hit for silicon?." Journal of Physics: Condensed Matter 24.16 (2012): 164201.

Huang, S., J. He, S. Chang, P. Zhang, F. Liang, S. Li, M. Tuchband, A. Fuhrmann, R. Ros, and S. Lindsay. "Identifying single bases in a DNA oligomer with electron tunnelling." Nature nanotechnology 5.12 (2010): 868-873.

Bath, J., and A. J. Turberfield. "Molecular machinery built from DNA." NOBEL SYMPOSIUM 153: NANOSCALE ENERGY CONVERTERS. Vol. 1519. No. 1. AIP Publishing, 2013.

Kim, T. Y., H. Kim, S. W. Kwon, Y. Kim, W. K. Park, D. H. Yoon, A.-R. Jang, H. S. Shin, K. S. Suh, and W. S. Yang. "Large-scale graphene micropatterns via self-assembly-mediated process for flexible device application." Nano letters 12.2 (2012):

743-748.

Lehn, J.-M. "Perspectives in ChemistrySteps towards Complex Matter." Angewandte Chemie International Edition 52.10 (2013): 2836-2850.

Pease, A. R., J. O. Jeppesen, J. F. Stoddart, Y. Luo, C. P. Collier, and J. R. Heath. "Switching devices based on interlocked molecules." Accounts of chemical research 34.6 (2001): 433-444.

Chang, S., J. He, P. Zhang, B. Gyarfas, and S. Lindsay. "Gap Distance and Interactions in a Molecular Tunnel Junction." Journal of the American Chemical Society 133.36 (2011): 14267-14269.

Wu, S., M. T. Gonzlez, R. Huber, S. Grunder, M. Mayor, C. Schnenberger, and M. Calame. "Molecular junctions based on aromatic coupling." Nature nanotechnology 3.9 (2008): 569-574.

Holmlin, R. E., R. F. Ismagilov, R. Haag, V. Mujica, M. A. Ratner, M. A. Rampi, and G. M. Whitesides. "Correlating electron transport and molecular structure in organic thin films." Angewandte Chemie 113.12 (2001): 2378-2382.

Slowinski, K., R. V. Chamberlain, C. J. Miller, and M. Majda. "Through-bond and chain-to-chain coupling. Two pathways in electron tunneling through liquid alkanethiol monolayers on mercury electrodes." Journal of the American Chemical Society 119.49 (1997): 11910-11919.

De Rege, P. J., S. A. Williams, and M. J. Therien. "Direct evaluation of electronic coupling mediated by hydrogen bonds: implications for biological electron transfer." Science 269.5229 (1995): 1409-1413.

Jeffrey, G. A. An introduction to hydrogen bonding. Vol. 12. New York: Oxford university press, 1997.

Scheiner, S. "Hydrogen bonding. A theoretical perspective." (1997).

Kim, K. S., P. Tarakeshwar, and J. Y. Lee. "Molecular clusters of -systems: theoretical studies of structures, spectra, and origin of interaction energies." Chemical reviews 100.11 (2000): 4145-4186.

Lee, E. C., D. Kim, P. Jurecka, P. Tarakeshwar, P. Hobza, and K. S. Kim. "Understanding of assembly phenomena by aromatic-aromatic interactions: benzene dimer and the substituted systems." The Journal of Physical Chemistry A 111.18 (2007): 3446-3457.

Tarakeshwar, P., and K. S. Kim. "Comparison of the nature of π and conventional H-bonds: a theoretical investigation." Journal of molecular structure 615.1 (2002): 227-238.

Gowacki, E. D., M. Irimia-Vladu, S. Bauer, and N. S. Sariciftci. "Hydrogen-bonds in molecular solidsfrom biological systems to organic electronics." Journal of Materials Chemistry B 1.31 (2013): 3742-3753.

Cahen, D., R. Naaman, and Z. Vager. "The cooperative molecular field effect." Advanced Functional Materials 15.10 (2005): 1571-1578.

Paltiel, Y., G. Jung, T. Aqua, D. Mocatta, U. Banin, and R. Naaman. "Collective effects in charge transfer within a hybrid organic-inorganic system." Physical review letters 104.1 (2010): 016804.

Janoschek, R., E.-G. Weidemann, H. Pfeiffer, and G. Zundel. "Extremely high polarizability of hydrogen bonds." Journal of the American Chemical Society 94.7 (1972): 2387-2396.

Eckert, M., and G. Zundel. "Proton polarizability, dipole moment, and proton transitions of an AH... B. dblharw. $A^-...H^+B$ proton-transfer hydrogen bond as a function of an external electrical field: an ab initio SCF treatment." Journal of Physical Chemistry 91.20 (1987): 5170-5177.

Natan, A., N. Kuritz, and L. Kronik. "Polarizability, Susceptibility, and Dielectric Constant of NanometerScale Molecular Films: A Microscopic View." Advanced Functional Materials 20.13 (2010): 2077-2084.

Moore, A. M., S. Yeganeh, Y. Yao, S. A. Claridge, J. M. Tour, M. A. Ratner, and P. S. Weiss. "Polarizabilities of Adsorbed and Assembled Molecules: Measuring the Conductance through Buried Contacts." ACS nano 4.12 (2010): 7630-7636.

Nishino, T., N. Hayashi, and P. T. Bui. "Direct Measurement of Electron Transfer through a Hydrogen Bond between Single Molecules." Journal of the American Chemical Society 135.12 (2013): 4592-4595.

Granhen, E. R., D. B. De Lima, F. M. Souza, A. C. F. Seridonio, and J. Del Nero. "Molecular electronic device based on pH indicator by ab initio and non-equilibrium Green function methodology." Solid-State Electronics 54.12 (2010): 1613-1616.

Lourderaj, U., K. Giri, and N. Sathyamurthy. "Ground and excited states of the monomer and dimer of certain carboxylic acids." The Journal of Physical Chemistry A 110.8 (2006): 2709-2717.

Allen, G., J. G. Watkinson, and K. H. Webb. "An infra-red study of the association of benzoic acid in the vapour phase, and in dilute solution in non-polar solvents." Spectrochimica Acta 22.5 (1966): 807-814.

Nakabayashi, T., H. Sato, F. Hirata, and N. Nishi. "Theoretical study on the structures and energies of acetic acid dimers in aqueous solution." The Journal of Physical

Chemistry A 105.1 (2001): 245-250.

Lee MH., OF. Sankey. J. Phys. Condens. Matter. 2009;21:351101.

Emberly, E. G., and G. Kirczenow. "Theoretical study of electrical conduction through a molecule connected to metallic nanocontacts." Physical Review B 58.16 (1998): 10911.

Tian, W., S. Datta, S. Hong, R. Reifenberger, J. I. Henderson, and C. P. Kubiak. "Conductance spectra of molecular wires." The Journal of chemical physics 109.7 (1998): 2874-2882.

Kemp, M., V. Mujica, and M. A. Ratner. "Molecular electronics: Disordered molecular wires." The Journal of chemical physics 101.6 (1994): 5172-5178.

Cohen, R., K. Stokbro, J. ML. Martin, and M. A. Ratner. "Charge transport in conjugated aromatic molecular junctions: Molecular conjugation and molecule-electrode coupling." The Journal of Physical Chemistry C 111.40 (2007): 14893-14902.

Perepichka, D. F., and M. R. Bryce. "Molecules with exceptionally small HOMOLUMO gaps." Angewandte Chemie International Edition 44.34 (2005): 5370-5373.

Ohashi, S., T. Iemura, N. Okada, S. Itoh, H. Furukawa, M. Okuda, M. Ohnishi-Kameyama, T. Ogawa, H. Miyashita, T. Watanabe, S, Itoh, H. Oh-oka, K. Inoue, M. Kobayashi. "An overview on chlorophylls and quinones in the photosystem I-type reaction centers." Photosynthesis research 104.2-3 (2010): 305-319.

Saito, K., A. W. Rutherford, and H. Ishikita. "Mechanism of proton-coupled quinone reduction in Photosystem II." Proceedings of the National Academy of Sciences 110.3 (2013): 954-959.

Zhang, Z., Z. Yang, J. Yuan, H. Zhang, Q. Ming, and X. Deng. "Electronic transport properties of pheny1 based molecular devices." Solid State Communications 149.1 (2009): 60-63.

Fan, Zhi-Qiang, and Ke-Qiu Chen. "First-principles study of side groups effects on the electronic transport in conjugated molecular device." Physica E: Low-dimensional Systems and Nanostructures 42.5 (2010): 1492-1496.

Zhang, Z., Z. Yang, J. Yuan, H. Zhang, Q. Ming, and X. Deng. "Electronic transport mechanism of a molecular electronic device: structural effects and terminal atoms." Physics Letters A 323.1 (2004): 154-158.

Olah, G. A. "Aromatic substitution. XXVIII. Mechanism of electrophilic aromatic substitutions." Accounts of Chemical Research 4.7 (1971): 240-248.